Megakaryopoiesis, Thrombopoiesis and the Microenvironment

Sijie Sun

A dissertation
submitted in partial fulfillment of the
requirements for the degree of

Doctor of Philosophy

University of Washington
2014

Reading Committee:
Dayong Gao, Chair
Ying Zheng
José López

Program Authorized to Offer Degree:
Bioengineering

University of Washington

Abstract

Megakaryopoiesis, Thrombopoiesis and the Microenvironment

Sijie Sun

Chairs of the Supervisory Committee:

Professor Dayong Gao
Department of Mechanical Engineering

Assistant Professor Ying Zheng
Department of Bioengineering

Bone marrow microenvironment has been suggested to be critical for platelet generation. Understanding the environmental cues that regulate megakaryocytes development and platelet production remains a major goal of developmental and clinical biology. My thesis projects focus on understanding interactions between bone marrow microenvironment and thrombopoiesis, so as to develop a novel method to produce platelets *in vitro*.

I first investigated soluble factors affecting megakaryopoiesis and thrombopoiesis by performing a genome-wide search to identify plasma membrane receptors whose ligands may play important functional roles in this developmental process. Thirty-night transmembrane receptor genes were identified. The robustness of this dataset was tested by selecting 7 receptor-associated genes and examining the ability of their matched-ligands to modulate megakaryocytopoiesis. Overall, 6 of 7 of the plasma membrane receptors have functional roles in megakaryocyte (MK) and platelet biology. These data also indicate for the first time that adiponectin plays a regulatory role in MK development. Most importantly, these results support the notion that there is a strong likelihood

that the 40 transmembrane genes constitute a MK receptome that will be an important resource to the research community for deciphering the complex repertoire of environmental cues that regulate megakaryocytopoiesis and/or modulate platelet function.

I also reconstituted an *in vitro* 3D microvascular niche, which allowed me to study the final maturation of MKs and the close interactions between MKs and endothelium. MKs migrate toward microvessels via CXCR4-mediated pathways, transmigrate across endothelium and release functional platelets into vessel lumen. I observed two transmigration modes: paracellular transmigration through cell-cell junction and pericellular transmigration directly through endothelial cells. Transmigration of MKs leaves pores in the endothelium and makes the microvessel leaky. This study suggests that big MK fragments may leave bone marrow and enter the blood steam. A stage of MKs with platelet territories was discovered in our study, indicating a transit stage between demarcation membrane system and proplatelet. Collectively, by developing 3D MK-microvessel coculture system, we successfully study the crosstalk between MKs and microvessel and produce and collect platelets from microvessel. This system would serve as an alternative human thrombopoiesis model, complementing animal models and clinical studies, and potentially serve as a platform for large-scale productions of platelets for transfusion.

Acknowledgements

I would like to express my sincere appreciation to all those who gave me the possibility to complete this dissertation. I am deeply indebted to my supervisors Drs. Dayong Gao and Ying Zheng for their guidance, encouragement and everything they have taught me in science and in life throughout these years. I have been very fortunate to have them as my mentors. I am heartily thankful to Dr. José López, whose insights, wisdoms, advices and enthusiasm for research have greatly influenced me and made the completion of this research work possible. I want to thank Dr. Jo-Anna Reems for introducing me into this research field and continuously help me wherever she is. I would also like to thank Drs. Buddy Ratner and Yong Tan for being on my committee and for all their valuable discussion at our meetings.

I thank all my labmates in the Gao lab and Zheng lab for helping me carry out experiments, providing me support and helpful discussions. I am obliged to Ping Luo, Quanhui Liu, Zhiquan Shu, Simon Chen, Surya Kotha, Jun Xue, Meredith Roberts, Giovanni Ligresti, Ryan Nagao, Dominic Tran, Katie Truong, Jin Xu, Yoon Jung Choi, Sameul Totorica, Cifeng Fang, Jiaji Pan, Xin Liang, Ruoxin Wang and Jinyuan Zhang.

I offer my regards and blessings to all of those at Puget Sound Blood Center who supported me in any respect during the completion of the project. I would like to thank Drs. Jing-Fei Dong, Junmei Chen, Wenjing Wang, Xiaoping Wu, Maria Nawrot, Adam Munday, Jennie Le, Teri Blevins, Jeff Harris, Maira Carrillo, Junli Feng for all the help and support.

Finally, I would like to give my special thanks to my parents, Jingxia Si and Zhimin Sun and my husband Weiping Ding. They have provided me with encouragements and given me

unconditional support. Finally, I would like to thank my daughter, Ava Ding, who has always brightened my day since the day she came to the world.

Table of Contents

Figures

Chapter 1 Introduction

1.1 Motivations and research objectives

Although only 100 years ago people considered platelets as the "dust of the blood", now the understanding of thrombopoiesis has grown rapidly and the importance of platelets is widely accepted. Human platelets, which are derived from bone marrow megakaryocytes, are small (~2.5um), plate-like anuclear cells. Approximately 150 billion platelets are produced every day in human adults at steady state [1]. In addition to their primary function of preventing and arresting hemorrhage, platelets also play important roles in regulating vascular integrity, angiogenesis, inflammation, and the immune response [2-4]. The importance of megakaryopoiesis and thrombopoiesis is apparent. Dysregulation of megakaryocyte development and platelet generation leads to severe thrombocytopenia with significant bleeding and mortality. About 2.5 percentage of normal population have got thrombocytopenia, which is a condition in which your blood has a lower than normal number of platelets [5]. The main causes of thrombocytopenia are decrease of platelets generation, increase of platelet destruction or trapping of platelets in the spleen [5]. Morbidity and mortality from bleeding due to moderate to severe thrombocytopenia are major problems facing a wide range of patients. One of the major treatments to severe thrombocytopenia is platelet transfusion. In the United States, approximately 1.5 million platelet transfusions are administered yearly to patients to reduce their risk of bleeding [1]. Unfortunately, platelet transfusion faces big problems. At least 30% of the transfusions are associated with medical complications, usually by immune or cytokine-mediated febrile reactions [1]. And platelet transfusions are expensive partially because the short storage time at room temperature and high risk of bacterial contamination.

Thus, a better understanding of megakaryopoiesis and thrombopoiesis and better strategies to treat severe thrombocytopenia and to accelerate platelet count are urgently needed. The goal of my PhD research is to understand the effect of microenvironment on thrombopoiesis and to develop a novel method to produce platelets *in vitro*. This objective is broken down into two sub-projects:

1.1.1 Identify novel soluble factors affecting megakaryopoiesis and thrombopoiesis.

Megakaryocyte (MK) development is critically regulated by plasma membrane-localized receptors that integrate a multiplicity of environmental cues. We performed a genome-wide search to identify plasma membrane receptors whose ligands may play important functional roles in this developmental process. Forty transmembrane receptor genes were identified. The robustness of this dataset was tested by selecting 7 receptor-associated genes and examining the ability of their matched-ligands to modulate megakaryocytopoiesis. Overall, 6 of 7 of the plasma membrane receptors have functional roles in MK and platelet biology. These data also indicate for the first time that adiponectin plays a regulatory role in MK development. Most importantly, these results support the notion that there is a strong likelihood that the 40 transmembrane genes constitute a MK receptome that will be an important resource to the research community for deciphering the complex repertoire of environmental cues that regulate megakaryocytopoiesis and/or modulate platelet function.

1.1.2 Investigate the megakaryocyte and microvessel interplay by developing a 3-D bone marrow niche biomimetic microdevice.

A 3-D microdevice has been developed to mimic bone marrow niche for thrombopoiesis, which contains microvessel network, extracellular matrix and bone marrow stromal. MKs have been co-cultured in the 3-D system with endothelial cells. We observed the migration and transmigration of MKs to microvessel, release of platelets into vessel lumen. We also first observed the MK-induced endothelial fenestration and sprouting angiogenesis. VEGF has been demonstrated to play a role in both endothelial fenestration and angiogenesis.

1.2 Background

1.2.1 Cellular origins of megakaryopoiesis and thrombopoiesis

Megakaryocytes (MKs), like other hematopoietic cells, are derived from hematopoietic stem cells (HSCs) in the bone marrow (Figure 1.1)[6]. Megakaryopoiesis can be divided into 4 stages[7]. The first stage is characterized by primitive HSCs capable of self-renewal. During MK maturation, HSCs give rise to different committed progenitor cells (stage 2), including colony forming units granulocytes, erythrocytes, monocytes, and megakaryocytes (CFU-GEMM), burst forming-MK (BFU-MK) and colony forming units-megakaryocytes (CFU-MK). The BFU-MK is a highly proliferative cell producing up to hundreds of MKs per cell while the CFU-MK, the more differentiated cell of the MK progenitors, produces about 3-50 cells per colony[1]. Intermediate between proliferating progenitor cells and mature MKs are the immature MKs (stage 3), including transitional pro-megakaryoblasts, megakaryoblast with a high nuclear to cytoplasmic ratio and promegakaryocyte with increased cytoplasmic volume and number of

platelet-specific granules. The final stage of MK development is the platelet-shedding megakaryocytes.

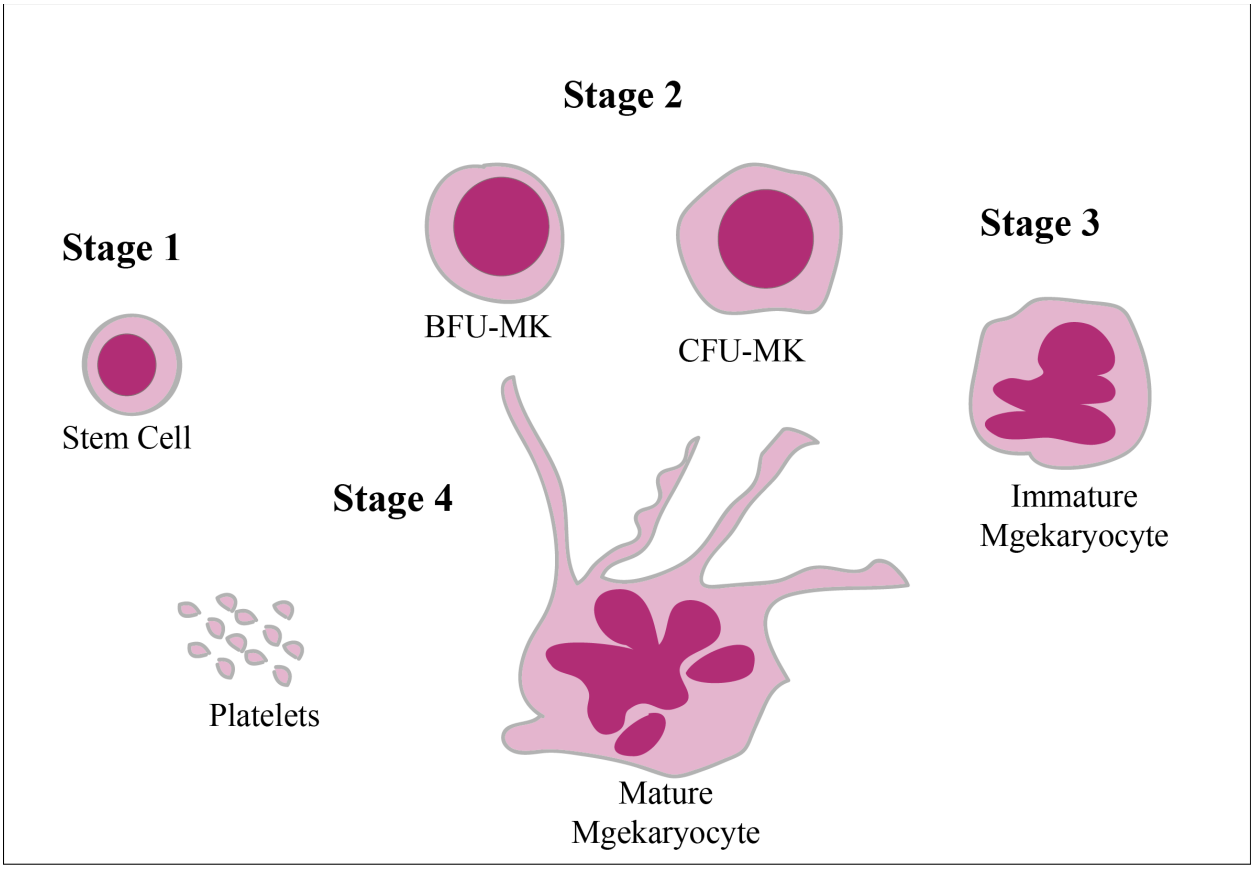

Figure 1.1 Overview of four stages of megakaryopoiesis.

Stage 1: Hematopoietic stem cells capable of self-renewal; stage 2: Committed megakaryocyte (MK) progenitors; stage 3: immature MKs; stage 4: platelet shedding MKs. Adapted from [7].

The mechanism of thrombopoiesis has been a matter of debate for several years. There are two models of thrombopoiesis. Proplatelet model and cytoplasm fragmentation model [8]. Proplatelet model proposed that mature MKs extend long, branching proplatelet into bone marrow sinusoid and release proplatelets or platelets into bloodstream. This model is supported by multiple ultrastructure images of proplatelets extending into bone marrow sinusoid [9, 10]. The cytoplasm

fragmentation model proposed that platelets are released by fragmentation of the cytoplasm without proplatelet formation. This model was supported by several electron micrographs of internal membrane of mature MKs [11, 12] and *in vitro* and *in vivo* observations of explosive fragmentation of the entire cytoplasm of MKs [13-15].

More evidence has indicated that in addition to bone marrow, lung might be another important location of thrombopoiesis. Lung is the first capillary bed entered by any cells leaving bone marrow [10]. Furthermore, MKs infused into mice by tail vein are mostly located to the pulmonary vasculature [16]. In human, 10 times more intact MKs are found in pulmonary arterial blood than in blood from aorta [17].

1.2.2 Bone marrow niche of megakaryopoiesis and thrombopoiesis

Bone marrow niche provides physical support, soluble factors and cell-mediated interaction to regulate the proliferation and maturation of MKs, and thrombopoiesis.

1.2.2.1 Soluble factors

Thrombopoietin (TPO) is the main regulator of MK development. It stimulates MKs to increase in cell size, ploidy and proplatelet formation [18]. In addition to TPO, other cytokines, including interleukin (IL) 3, IL6, IL11, stem cell factor (SCF), Fms-like Tyrosine Kinase-3 (FLT3), fibroblast growth factor (FGF) and erythropoietin (EPO) have also been reported to stimulate megakaryopoiesis alone or combined with TPO [8, 14, 19]. Transforming growth factor β1 (TGF β1)[20], platelet factor 4 (PF4) [21] and IL4 [22] are negative regulators of megakaryopoiesis [8].

Stromal cell-derived factor 1(SDF1), whose main receptor is CXCR4, is a key chemokine involved in hematopoietic cells in bone marrow. SDF1 is synthesized mainly by bone marrow stromal cells, endothelial cells, MKs and dendritic cells [23, 24]. SDF1 and FGF-4 restore

platelets production in TPO-/- and c-mpl-/-. SDF1 enhances the MK movement to junctions between sinusoid, while FGF-4 promote the adhesion of MK to bone marrow endothelial cells [25].

1.2.2.2 Non-cellular factors in the bone marrow niche

Oxygen tension. MKs grow and mature in proximity to the BM sinusoid. Platelet shedding occurs either in BM sinusoid or lung vasculature, where oxygen tension is relative higher than BM endosteal niche where HSCs reside. Peripheral blood CD34+ cells produced more CD41+ cells [26] and CD41+ cells and yielded higher ploidy MKs [26] under 20% pO_2 than under 5% pO_2. In contrast, More CFU-MK was produced under 5% pO_2 [27], indicating mature MKs prefer higher oxygen tension, while MK progenitors prefer lower oxygen tension.

Shear force. Human mature MKs were perfused at a high shear rate on von Willebrand factor (VWF) coated surface. Higher percentage of proplatelets and platelets was formed [28].

Extracellular matrix in bone marrow niche. Extracellular matrix proteins are the main component of bone marrow niche. Vitronectin, collagen [29], VWF [30] and fibrinogen [31] have been shown to promote proplatelet formation. GPIIb/IIIa and GPIb both play a role in thrombopoiesis. Mutation of GPIIb/IIa induced proplatelet formation in the presence of fibrinogen [32]. GPIb deficiency in human or mice causes thrombocytopenia with an increased size of platelets [33, 34].

1.3 *In vitro* production of platelets

Platelets have been reported to be produced from different sources of HSCs: human cord blood derived stem cells [35-39], bone marrow derived stem cells[40, 41], mobilized peripheral blood derived stem cells[42, 43] and embryonic stem cells[44, 45].

2-step strategy was mostly used for large amount production of platelets [38-40, 42, 43]. HSCs, with or without stromal cells, were cultured in one culture condition to promote proliferation. After 3-10 days culture, cells were moved to another culture condition with different cytokine combination to facilitate differentiation of MKs. Some groups added one more step to enhance the terminal differentiation of MKs and release of platelets [37].

In addition to traditional 2D culture, 3D bioreactors were also developed to facilitate platelet production. Sullenbarger *et al* grew cord blood CD34+ cells in surgical-grade woven polyester fabric or hydrogen scaffolds and continuously produce platelets for more than 32 days [46]. Pallotta *et al* developed a 3D bioreactor using a silk-based vascular tube and generate platelets from cord blood stem cells [47].

In order to characterize culture derived platelets, most of the studies tested platelet-specific surface markers (CD41, CD42b), fibrinogen binding and morphology change and P-selectin expression change with agonist. Although these studies indicated that culture derived platelets share similar morphological and functional characteristics with human nature platelets, no *in vivo* assay has been performed to test their hemostatic function.

Because of the low yield of platelet production and questionable quality of culture derived platelets, another strategy was also been studied to replace standard platelet products: expanding MKs instead of platelets *in vitro*. Infusion of murine mature MKs into mice yield function

platelets [16]. Human cord blood derived megakaryocytic progenitors has been infused into patients with advanced hematological malignancies [48]. With one year follow-up, acute and chronic GVHD had not been observed among patients, even without ABO blood group and HLA typing matching. These initial results suggested that infusion of megakaryocytic progenitors appears safe and feasible for treatment of thrombocytopenia.

Chapter 2 Establishment of an *in vitro* megakaryopoiesis and thrombopoiesis culture system

2.1 Abstract

One of the main therapies for severe thrombocytopenia is platelet transfusion. However, platelet transfusion is not ideal due to the related medical complications, cost and consumed time. Researchers tried to develop alternative methods to treat sever thrombocytopenia. One of them is to produce functional platelets from hematopoietic stem cells. Although several publications indicated the success, the quality of produced platelets has not been confirmed. In this chapter, I established an *in vitro* culture system to obtain megakaryocytes (MKs) and platelets. Interleukin (IL) 3, IL6, stem cell factor (SCF) and thrombopoietin (TPO) were used as a cytokine cocktail to enhance both proliferation of stem cells and differentiation of stem cells into MK lineage. Proplatelet formation was achieved by culturing MKs on VWF-coated surface. Although the differentiation of cord blood CD34+ cells into MKs occurs efficiency, terminal maturation of MKs appears to be precluded. Cord blood CD41+ platelet-like particles could be obtained from culture supernatant, but the number of platelets produced by each MK was low. Although the limitation of the 2-D suspension culture system requires better culture system to produce functional platelets, it still can be used as a platform to produce MKs and platelets *in vitro* for further research.

2.2 Introduction

In the United States, approximately 1.5 million platelet transfusions are administered yearly to patients to reduce their risk of severe bleeding and the demand is steady increasing[49]. However,

the platelet transfusion therapy is way from ideal. It is expensive, time-consuming and of limited efficacy. Thus an alternative therapy is urgently needed. One of the solutions is to produce platelets of clinical quality *in vitro* for transfusion. Hematopoietic stem cells from bone marrow, peripheral blood, umbilical cord blood and embryonic stem cells have been cultured and differentiated into MKs successfully[7]. Most of the culture system uses a two-stage strategy: first stage to amplify hematopoietic stem and progenitors, the second stage to differentiate them into MKs[7]. Although a number of studies indicate that platelets produced in vitro have a similar morphology, surface markers and function as blood platelets. A considerable portion of produced particles is cell debri from MKs, activated platelets or non MK cells. In this chapter, I would introduce a culture strategy to produce MKs and platelets from cord blood. This strategy would be the platform to generate MKs for research and for the following chapters.

2.3 Materials and Methods

2.3.1 Cytokines and antibodies

Recombinant human cytokines interleukin (IL) 3, IL6, SCF were purchased from R&D Systems (Minneapolis, MN). Phycoerythrin (PE) conjugated anti-human antibodies CD41a and mouse IgG1 isotype control were purchased from BD biosciences (San Jose, CA, http://www.bdbiosciences.com). Human VWF was purified from commercial cryoprecipitate prepared at Puget Sound Blood Center as described in [50].

2.3.2 Enrichment of human cord blood CD34+ cells

Human umbilical cord blood (UCB) was donated after obtaining informed consent. UCB was processed by adding 6% (wt/vol) Hetastarch (Hospira, Lake Forest, IL) to a final concentration

of 1.2%, and gravity sedimented over 60 min. [51] The leukocyte-enriched supernatant was removed, centrifuged for 10 min at 300 x g, and the leukocyte-poor supernatant was removed. The cell pellet was treated with ACK lysing buffer (Invitrogen, Carlsbad, CA), followed by a wash with PBS. To obtain highly purified CD34+ cells, leukocyte-enriched fractions were labeled with anti-CD34 antibody conjugated to magnetic microbeads (Miltenyi Biotec, Bergisch Gladbach, Germany). CD34+ cells were positively selected with an autoMACS separator according to the manufacturer's instruction. Greater than 90% of the enriched cells were CD34+ cells as determined by flow cytometry (FACSCaliber; Becton Dickinson).

2.3.3 Culture derived megakaryocytes

UCB CD34+ cells were seeded at a density of $5x10^4$ cells/ml and cultured in serum-free X-vivo 10 medium supplemented with a cytokine combination consisting of IL3 (10 ng/ml), IL6 (10 ng/ml), SCF (10 ng/ml), and TPO (50 ng/ml) (Day 0). The suspension cultures were incubated and fed every week at 37^oC in a 5% CO_2 humidified chamber.

2.3.4 Surface marker expression by flow cytometry

Cells were collected by centrifugation and re-suspended into phosphate-buffered saline (PBS)/2% Bovine Serum (BS). Cells were then stained with FITC or PE conjugated antibodies, or the corresponding isotype controls and incubated for 15 minutes. Cells were washed and analyzed on a FACSCalibur flow cytometer. For indirect labeling, after labeling cells with a primary antibody, cells were stained with a FITC or PE conjugated secondary antibodies. Cells were then analyzed on a FACSCalibur flow cytometer.

2.3.5 Proplatelet formation

UCB CD34+ cells were cultured in serum-free X-vivo 10 medium supplemented with a cytokine combination consisting of IL3 (10 ng/ml), IL6 (10 ng/ml), SCF (10 ng/ml), and TPO (50 ng/ml) for 7 days. Day 7 cells were stained with FITC conjugated anti-CD41 antibody and CD41+ cells were sorted by BD FACSCalibur cell sorter (San Jose, CA). CD41+ cells were then placed on 12-well plate containing a VWF coated glass coverslip.

2.4 Results

2.4.1 Differentiation of megakaryocytic lineage cells

A cytokine combination – interleukin (IL) 3 (10ng/ml), IL6 (10ng/ml), stem cell factor (SCF) (10ng/ml) and thrombopoietin (TPO) (50ng/ml)- was used to generate MKs from CB CD34+ cells. After 10 days culture, the total nucleated cells number was increased by 24 times, and 74% ± 9% of cells expressed CD41 antigen which is the specific surface maker for MKs. There are clearly two populations of MKs based on the expression level of CD41 antigen and cell size (forward scatter) according to flow cytometry analysis (Figure 2.1A). Most of the CD41+ MKs expressed CD41 antigen at lower lever and remained smaller at day 5, while higher CD41expressing larger MKs started occurred at approximately day 8. The percentage of highly CD41 expressed larger MKs is increased during the incubation, indicating that MKs in culture become more mature. To optimize the culture condition, we compared two cytokine combination – IL3 (10ng/ml), Il6 (10ng/ml), SCF (10ng/ml), TPO (50ng/ml) (36ST) and IL6(10ng/ml), SCF(10ng/ml), TPO(50ng/ml), Flt 3(10ng/ml) (6STF). CB CD34+ cells were cultured with each of the two cytokines for 16 day. Cells were fed each week and CD41 antigen expression was analyzed every day since day 5. The maximum percentage of cells expressing

low quantities of CD41+ was 53% ± 0.7% and 72% ± 2% when CB CD34+ cells were cultured with 36ST or 6STF respectively, both occurring on day 15 (Figure 2.1B). Highly CD41 expressed cells reached the maximum percentage on day 11 (19% ± 1%) and day 12 (27% ± 2%), when CB CD34+ cells were cultured with 36ST or 6STF respectively (Figure 2.1B).

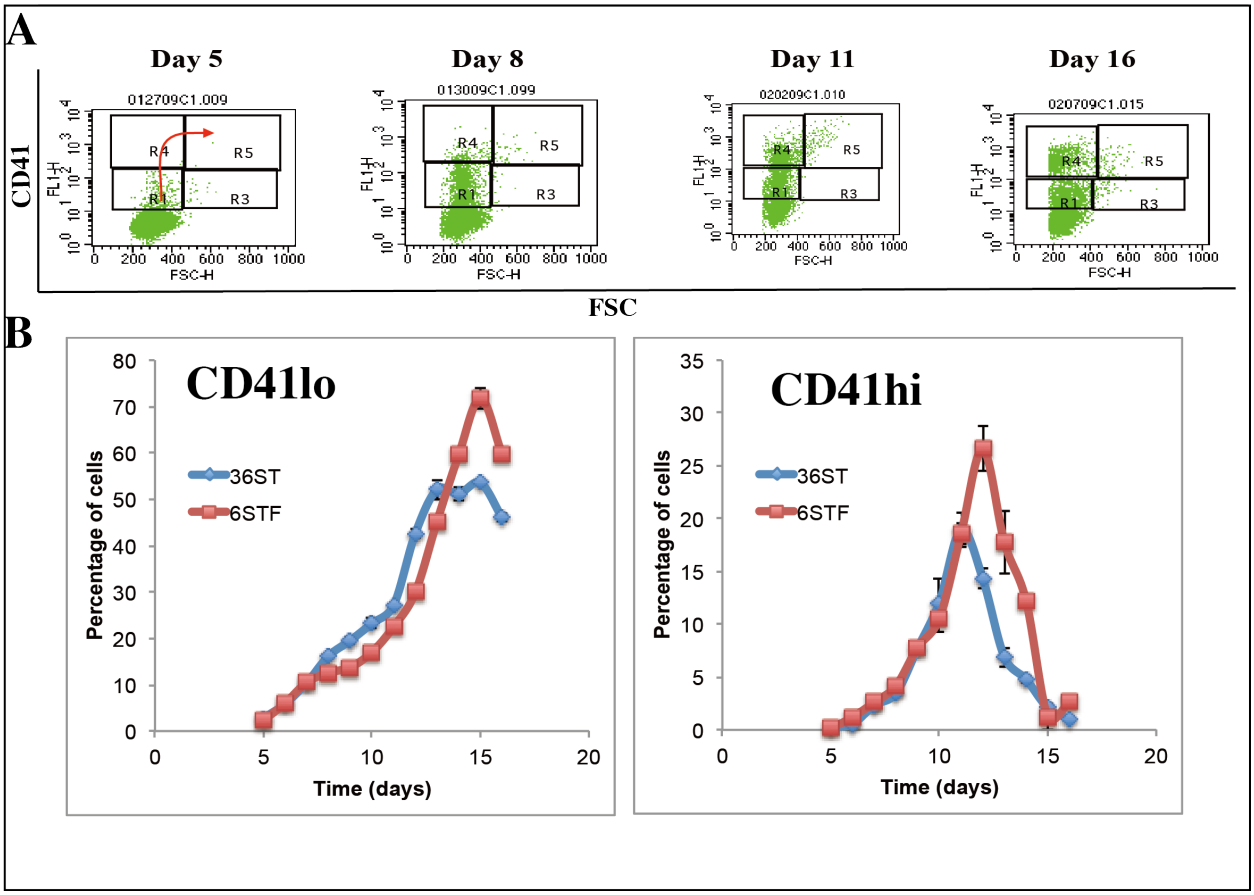

Figure 2.1 Kinetics of *in vitro* megakaryocytes (MK) development.

(A) The flow cytometry dot plots compare CD41 expression and FSC during MKs development. (B) Percentage of $CD41^{lo}$ (left) expression and $CD41^{hi}$ (right) expression during MKs development. N=3.

2.4.2 Generation of platelet-like particles from in vitro culture

Small particles released from culture derived MKs were collected and analyzed (Figure 2.2A). FACS analysis data of plasma-derived fresh platelets from the healthy volunteers is shown in Figure 2.2B. Gate 1 was considered as platelet-sized particles. Only CD41+ gate 1 particles were considered as platelet-like particles (PLP), while the other CD41- particles were surmised to be cell debris. The number of CD41+ platelet-sized particles (platelet-like particles) was compared to mature CD41hi megakaryocytes (cells in gate R4 and R5 as in Figure 2.1A). Approximately 76, 45 and 6 platelet-like particles were released from each mature megakaryocyte on days 10, 12 and 14, respectively (Figure 2.2C).

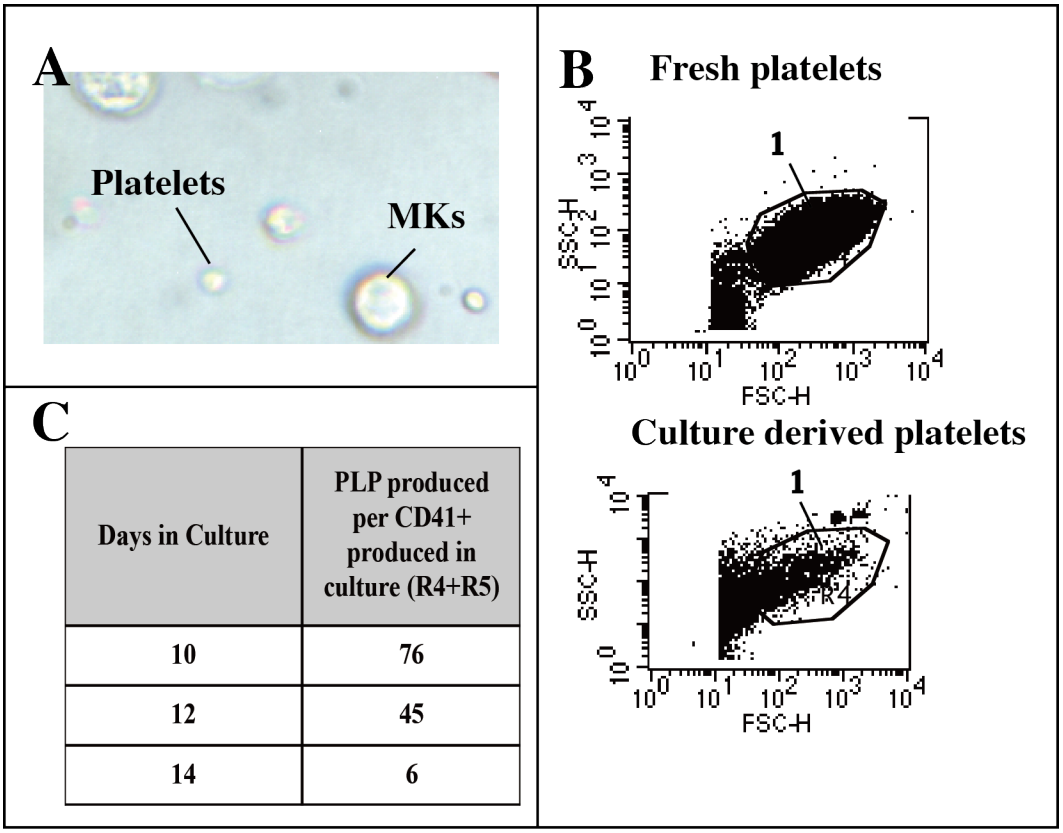

Days in Culture	PLP produced per CD41+ produced in culture (R4+R5)
10	76
12	45
14	6

Figure 2.2 Platelet-like particles (PLP) released from *in vitro* megakaryocyte (MK) culture.

(A) Light micrograph of MKs and released PLPs. (B) The flow cytometry dot plots compare human fresh platelets and *in vitro* culture derived PLPs. (C) PLPs produced per CD41+ cells produced in culture.

2.4.3 Generation of proplatelet

MKs tend to be suspended in 2-D culture system. Thus few proplatelets could be observed. However, MKs could attach to a surface coated with extracellular matrix, which promoted proplatelet formation.[30] Here human von Willebrand brand factor (VWF) was used to be coated on a glass coverslip to allow MK attachment. Day 7 CD41+ MKs were cultured on a VWF coated surface for another 7 days. Approximately 20% of MKs formed proplatelets (Figure 2.3). The culture derived proplatelets have the hallmark feathers of human proplatelets – long, thin shafts, branch points and swelling tips (Figure 2.3A, C, D). The Wright – Giemsa staining also showed the very thin cytoplasmic coverage around nuclei of proplatelet forming MKs (Figure 2.3B).

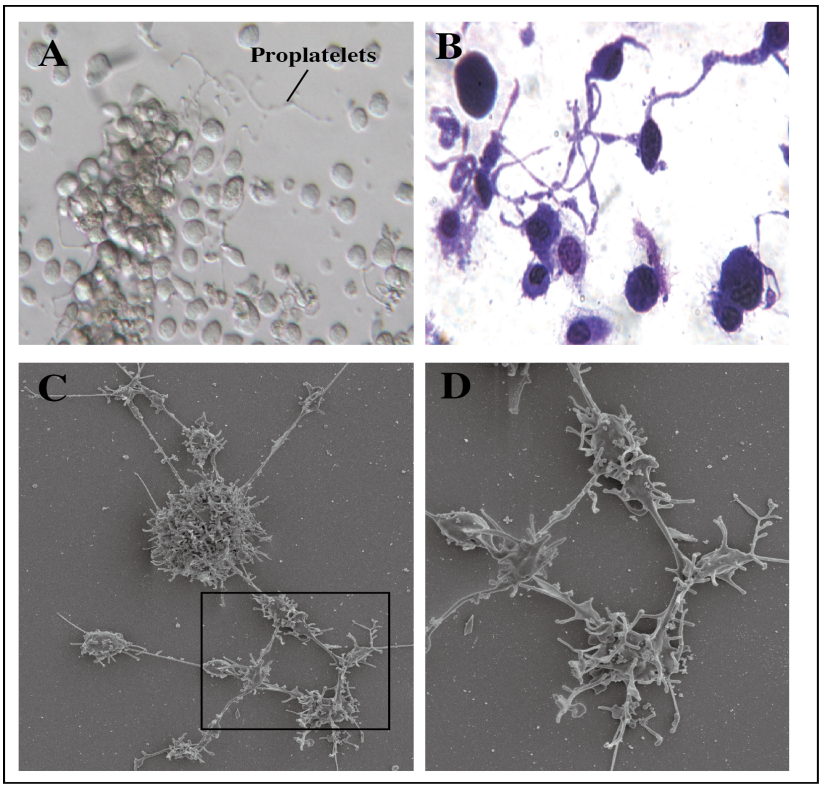

Figure 2.3 Proplatelet formation on VWF coated surface.

(A) Light micrograph of proplatelets after 14 days culture on VWF coated glass. (B) Wright-Giemsa stain of proplatelets. (C) Scanning electron micrograph (SEM) of a proplatelet forming megakaryocyte. (D) Zoomed SEM of proplatelets.

2.5 Discussion

In this chapter, I demonstrated a 2-D culture system to generate MKs and platelets using serum-free media and a cytokine combination. Approximately 20 times more nucleated cells could be obtained on day 10 compared to the seeded CD34+ cells. 73% of the day 15 cells were expressing CD41 antigen when cells were cultured with IL6, SCF, TPO and FLT3. CD41+ platelets-like particles could be obtained in the supernatant of culture-derived MKs from CB. Proplatelet formation was observed from UCB culture derived MKs. These results imply that our

method of MKs and platelets generation could be feasible for a platform to study megakaryopoiesis and thrombopoiesis.

Although the 2-D culture system could be used to generation platelets, the limitation of it is apparent: (a) the ploidy of culture derived MKs is low. (Data not shown) Even for $CD41^{hi}$ MKs, most of them are still low ploidy (2N-4N). However, in vivo 80% of the low ploidy (4N-8N) MKs were immature and 95% of the platelet shedding megakaryocytes were 16N-32N.[52] (b) Culture generated platelets from each MK are few, only approximately 76 platelets from each MK, compared to 1000 to 3000 platelets from each MK *in vivo*.[53] (c) the number of culture generated MKs was not high enough for large scale production in clinic.

It has been always a problem that cord blood derived MKs have lower ploidy. Although cord blood CD34+ cells give rise to approximately 10-fold more MKs than peripheral blood (PB) derived CD34+ cells, MKs generated from CB are always smaller and of lower ploidy than peripheral blood derived MKs. [54] Proplatelets produced from CB MKs are also smaller, with fewer branches and bulbs than PB MKs derived proplatelets. [54] However, unlike BM MKs, the maturation and polyploidization of which appear to be linked [53], 58% of low-ploidy CB MKs (2N and 4N) are already cytoplasmically mature. [54] Not only in *in vitro* culture, after human CB transplantation, MKs in the postengraftment BM samples were significantly smaller than that after BM transplantation. [55] Similarly, these small MKs have a lower DNA content, but mature-appearing cytoplasm. As a reflection of the smaller size and smaller cytoplasmic volume, CB MKs also produce fewer platelets [56, 57], which explained why each of our culture derived MK produce only about 76 platelets, compared to 1000 to 3000 platelets from each MK *in vivo*.[53]

Cord blood has been demonstrated to be a good source for hematopoietic stem cells, and is used for stem cell transplantation and *in vitro* platelet generation. However, cord blood transplantation faces delayed platelet engraftment and *in vitro* platelet production faces fewer platelets derived from each MKs. What is the mechanism behind them? Slayton et al transplanted mice newborn liver hematopoietic stem cells and adult bone marrow stem cells into recipient mice. [58] They found that transplanted stem cells, regardless of their sources, gave rise quickly to big MKs that were even larger than normal adult MKs. However, MKs derived from neonatal stem cells were significantly smaller than those derived from adult bone marrow stem cells. These results indicated that both intrinsic and microenvironmental factors contribute to the difference of generating large MKs between neonatal and adult stem cells. In human clinical study, the median MKs diameter seen in patients after CB transplantation (16.7 μm) [55] is between the mean diameter of neonatal MKs (15.3 μm) and adult MKs (19.4 μm) [59], which also supported that microenvironment plays a role in regulating CB MKs size along with intrinsic factors.

In summary, although our technology to produce human MKs and platelets from CB in vitro is not sufficient for large-scale production of platelets for clinic use, it could still be a good platform to study MKs and platelets. To further improve the ability to produce large scale of platelets from CB, both intrinsic and microenvironmental factors should be considered and optimized. In the next chapter, a systematic method was used to screen and find novel soluble factors affecting MKs development, and in chapter 4 and 5, a 3-D biomimetic microdevice has been developed to mimic bone marrow niche for thrombopoiesis and try to find possible factors to improve thrombopoiesis.

Chapter 3 Investigation of the expression of plasma membrane receptor during megakaryocyte development

3.1 Abstract

Megakaryocyte (MK) development is critically informed by plasma membrane-localized receptors that integrate a multiplicity of environmental cues. Since current understanding about receptors and ligands involved in megakaryocytopoiesis has been based on single targets, we performed a genome-wide search to identify plasma membrane receptors whose ligands may play important functional roles in this developmental process. Thirty-nine transmembrane receptor genes were identified as being up-regulated during MK development. The robustness of this dataset was tested by selecting 7 receptor-associated genes and examining the ability of their matched-ligands to modulate megakaryocytopoiesis. These genes included: interleukin 9 receptor (IL9R), transforming growth factor, β receptor II (TGFBR2), interleukin 4 receptor (IL4R), colony stimulating factor-2 receptor-beta (CSFR2B), adiponectin receptor (ADIPOR2), thrombin receptor (F2R), and interleukin 21 receptor (IL21R). RNA and protein analyses confirmed their expression in primary human MKs. Matched-ligands to IL9R, TGFBR2, IL4R, CSFR2B, and ADIPOR2 affected megakaryocytopoiesis. IL9 was unique in its ability to increase the number of MKs formed. In contrast, MK colony formation was inhibited by adiponectin, TGFβ, IL4, and GM-CSF. The thrombin-F2R axis affected platelet function, but not MK development, while IL21 had no detectable effect on platelet function or MK development. Overall, 6 of 7 of the plasma membrane receptors have a functional role in MK and platelet biology. These data also indicate for the first time that adiponectin plays a regulatory role in MK development. We anticipate that the MK receptome defined in this study will be an important

resource to the research community for deciphering the complex repertoire of environmental cues that regulate megakaryocytopoiesis.

3.2 Introduction

Megakaryocytopoiesis involves the proliferation and differentiation of hematopoietic stem cells to form MK progenitors that undergo a maturation process that culminates in a release of approximately 10^{11} platelets per day into the blood circulation [60]. This process is tightly regulated by a number of factors, which include extracellular cues such as cytokines, cell-to-cell interactions, and cell-to-extracellular matrix interactions. Among cytokines that are known to act as important extracellular regulators of megakaryocytopoiesis is the main physiological stimulator of this specific cell-lineage commitment, thrombopoietin (TPO) [1]. Additionally, interleukin 3 (IL3), interleukin 6 (IL6), interleukin 11 (IL11), stem cell factor (SCF) and fms-like tyrosine kinase 3 ligand (FLT3) act as positive regulators of MK development [1, 60]. There are also several cytokines which are documented as negative regulators of MK development, such as transforming growth factor beta (TGFβ), platelet factor 4 (PF4) and interleukin 4 (IL4) [60].

The importance of megakaryocytopoiesis and platelet biogenesis is apparent; morbidity and mortality from bleeding due to moderate to severe thrombocytopenia is a major problem facing a wide range of patients. An effective treatment to combat bleeding disorders is the transfusion of allogeneic platelets into patients with low platelet numbers and/or functionally defective platelets. However, because platelet products have a short shelf-life and because there is also a high demand for their use in transfusion settings, it is not uncommon for medical facilities to experience shortages of transfusable platelets. Consequently, achieving a readily available and

constant supply of allogeneic platelets for transfusion purposes continues to be a challenging endeavor for blood banks.

Platelet shortages may one day be alleviated through clinical scale *in vitro* production of platelets from stem cells. Efforts to achieve such an endeavor are currently underway, but despite the progress made the number and quality of platelets produced *in vitro* are inefficient [7]. As a result, it is still not feasible to produce large enough numbers of functional MKs to be able to generate platelets in quantities that are needed for clinical applications [1]. A key to successfully achieve this endeavor will require knowing how to regulate an artificial environment that supports platelet biogenesis. This will require a comprehensive understanding about the complex nature of the numerous environmental cues that facilitate the proliferation, differentiation, maturation and release of platelets.

In view of the fact that receptors found on the surface of a cell are responsible for integrating a multiplicity of environmental cues to instruct cells to perform biological responses (i.e. divide, differentiate, die), the objectives of this study were to use a systems biology approach to generate a map of receptors that are up-regulated during the development of human MKs and to validate the robustness of the dataset. This list of receptor-associated gene is composed of genes that are well documented as playing a role in MK development and platelet biology and a number of other genes that have no prior association with this lineage. The strength of this dataset indicates that it should be useful for identifying novel ligand-receptor systems that play functional roles in MK development.

3.3 MATERIALS AND METHODS

3.3.1 Cytokines and antibodies

Recombinant human cytokines IL3, IL6, SCF, interleukin 21 (IL21), interleukin 9 (IL9), thrombin, TGFβ, IL4, granulocyte/macrophage-colony stimulating factor (GM-CSF) and adiponectin were purchased from R&D Systems (Minneapolis, MN). Phycoerythrin (PE) conjugated anti-human antibodies CD41a, CD61 and FITC conjugated anti-human CD61 were purchased from BD biosciences (San Jose, CA, http://www.bdbiosciences.com). PE conjugated anti-human antibodies to IL9R, TGFBR2, and CSF2RB, and allophycocyanin (APC) conjugated anti-human antibodies to IL4Ra, and IL21R were purchased from R&D Systems. Anti-human antibodies F2R was obtained from R&D and anti-human ADIPOR2 was purchased from ABBIOTEC (San Diego, CA). Rabbit anti-goat IgG, goat anti-mouse IgG1, and goat IgG isotype controls were purchased from Southern Biotech (Birmingham, AL). Mouse IgG1 isotype control was purchased from eBioscience (San Diego, CA).

3.3.2 Purification of human bone marrow (BM) CD34+/CD38^{lo} cells

Institutional Review Board approval was obtained for the isolation and purification of human progenitor cells. Briefly, after obtaining informed consent from the families of organ donors, total nucleated cells (TNCs) ($42.1\pm6.80\times10^9$; mean±SEM) were obtained from vertebral bodies procured by Northwest Tissue Services (Seattle, WA) [61]. TNCs were applied to an Isolex 300 SA (Nexell, Irvine, CA) column to yield on average of $22.4\pm2.95\times10^7$ CD34+ cells with purities of 87±3.4% as determined by flow cytometry. Enriched fractions of CD34+ cells were subsequently frozen and stored in 1 ml aliquots containing $5\text{-}10\times10^6$ cells per vial at –135 ^{o}C in X-vivo 10 (Lonza, Walkersville, MD) medium containing 10% dimethyl sulfoxide (Research

Industries Corporations, Salt Lake City), 20% HyClone bovine serum (Invitrogen Corp., Carlsbad, CA) and 2mM L-glutamine (Invitrogen Corp.).

To isolate highly purified populations of CD34+/CD38^{lo} cells, aliquots of frozen CD34+ cells were thawed rapidly at 37^{o}C and co-stained with antibodies directed against CD34 and CD38 antigens. Adult marrow CD34+ cells were sub-populated based on co-expression of CD38 using a FACSVantage flow cytometer (Becton Dickinson, San Jose, CA) to obtain a CD34+/CD38^{lo} population of cells with >95% purity.[62]

3.3.3 Purification of human umbilical cord blood (UCB) CD34+ cells

Human UCB was donated after obtaining informed consent. UCB was processed by adding 6% (wt/vol) Hetastarch (Hospira, Lake Forest, IL) to a final concentration of 1.2% [51], and gravity sedimented over 60 min. The leukocyte-enriched supernatant was removed, centrifuged for 10 min at 300 x g, and the leukocyte-poor supernatant was removed. The cell pellet was treated with ACK lysing buffer (Invitrogen, Carlsbad, CA), followed by a wash with PBS. To obtain highly purified CD34+ cells, leukocyte-enriched fractions were labeled with anti-CD34 antibody conjugated to magnetic microbeads (Miltenyi Biotec, Bergisch Gladbach, Germany). CD34+ cells were positively selected with an autoMACS separator according to the manufacturer's instruction. Greater than 90% of the enriched cells were CD34+ cells as determined by flow cytometry (FACSCaliber; Becton Dickinson).

3.3.4 Culture derived megakaryocytes

Purified populations of marrow CD34+/CD38^{lo} cells or UCB CD34+ cells were seeded at a density of 5x10^{4} cells/ml and cultured in serum-free X-vivo 10 medium supplemented with a cytokine combination consisting of IL3 (10 ng/ml), IL6 (10 ng/ml), SCF (10 ng/ml), and TPO

(50 ng/ml) (Day 0).[41] The suspension cultures were incubated for 10 days at 37^{o}C in a 5% CO_2 humidified chamber.

3.3.5 Isolation of total RNA and cDNA synthesis

According to manufacturer's instructions (RNAeasy kit (QIAGEN inc., Valencia, CA)), RNA was isolated from uncultured cells, culture-derived MKs and other indicated cell types. Isolated RNA was stored at -80^{o}C until use. Total RNA (2 mg) from each sample was reverse transcribed into cDNA using Qiagen Omniscript™ according to the manufacturer's protocol.

Microarrays- As we previously published [61], microarray analysis of uncultured CD34+/CD38^{lo} cells and culture derived MKs was performed according to the manufacturer's instructions (Affymetrix Inc., Santa Clara, CA). Briefly, the quantity and purity of total RNA was analyzed using UV spectrophotometry and the integrity of intact total RNA was verified. Biotin-labeled target cRNA was prepared from 8 mg of total RNA from each sample and hybridized to Human Genome U133A and U133B Affymetrix GeneChips® (Affymetrix Inc., Santa Clara, CA). The hybridized chips were washed and stained with streptavidin phycoerythrin solution, then scanned at a wavelength of 570nm using an Affymetrix HP GeneArray™ Scanner (Santa Clara, CA).

Microarray data were analyzed using Rosetta Resolver® Expression Data Analysis System (Resolver) (Rosetta Biosoftware, Kirkland, WA), which utilizes an error-modeling-based approach verified through self-versus-self experiments, rather than the non-parametric statistical method of MAS 5.0 (http://www.rosettainpharmatics.com/products/resolver/default.htm). The calculation of statistical confidence (p-value) was derived from the total calculated error consisting of both random and systematic error. Gene expression profiles of significantly changed transcripts were then generated using a fold change cut-off of > 1.5 and a p-value of <

0.01. Profiles from each of three biological replicate experiments were intersected to attain a set of reproducible genes.

3.3.6 Megakaryome and Genome Receptome enrichment gene list

To define a list of training genes that make-up the megakaryome, we used the Toppgene database (http://toppgene.cchmc.org/) [63]. To derive this list, genes were identified from mouse and human gene ontology annotations, pathway associations, and those that have been observed in mouse gene knockout models that cause abnormal megakaryocyte development or abnormal platelet function. Receptors localized to the plasma membrane were identified using the Human Plasma Membrane Receptome database (Http://Receptome.Stanford.edu) [64].

3.3.7 Semi-Quantitative Reverse Transcriptase-Polymerase Chain Reaction

Total RNA (100 ng) from uncultured or cultured-derived MKs was reverse transcribed into cDNA using the SuperScript III First-Strand Synthesis Kit (Invitrogen, Carlsbad, CA) and PCR was performed using Platinum Taq DNA polymerase (Invitrogen). The thermocycling program consisted of: denaturation at 95°C for 10 s, followed by 40 cycles of PCR (95°C for 10 s, 55°C for 5 s, 72°C for 10 s) and an additional incubation for 10 min at 72°C. In each case, product identity was demonstrated by the presence of a single band of the appropriate size when analyzed by electrophoresis on a 1% agarose gel.

3.3.8 Western Blot Analysis

Cells were lysed in Cell Disruption Buffer using the PARIS kit (Applied Biosystems/Ambion). Protein concentrations were determined using a Pierce Coomassie Plus-The Better Bradford Assay Kit (Thermo Fisher Scientific, Rockford, IL). 20μg of protein from each sample was

mixed in NuPage LDS (Invitrogen, Carlsbad, CA), heated to 99^{o}C for 5 minutes, and electrophoresed after loading onto a 4-15% Ready Gel Tris-HCI Gel (Bio-Rad Laboratories, Inc., Hercules, CA). Separated proteins were transferred to PVDF Membrane (Bio-Rad Laboratories, Inc., Hercules, CA), which were probed with anti-ADIPOR2 antibody diluted 1/400 followed by a goat protein A-horseradish peroxidase (HRP) conjugate diluted 1/3000 (Bio-Rad Laboratories, Inc., Hercules, CA). Immunoreactive bands were visualized using a Western Lighting plus-ECL kit (PerkinElmer, Waltham, MA).

3.3.9 Platelet immunophenotyping and aggregation studies.

For immunophenotyping, 7 volumes of human whole blood was drawn into one volume of anticoagulant citrate dextrose solution A (Citra Anticoagulant, Inc., Braintree, MA) and centrifuged at 120g for 10min with the centrifuge brake in the off mode. The top layer or platelet rich plasma (PRP) was removed and centrifuged at 1,200g for 10min. The supernatant was removed and the platelet pellet was resuspended in citrate-glucose-saline buffer containing 120 mM sodium chloride, 13 mM sodium citrate and 30mM glucose buffer prior to labeling with antibodies for flow cytometry or for preparing a cell lysate for Western Blot analysis.

For aggregation studies, human whole blood was drawn into 3.2% sodium citrate and centrifuged at 120g for 10 min and the PRP was transferred into a fresh tube. The remaining whole blood was again centrifuged at 2000g for 10min to obtain a platelet poor plasma (PPP) fraction. Using the PPP, the platelet count of the PRP was adjusted to 250,000 platelets/ml. Percent aggregation was determined using an AggRAM aggregometer (Helena Laboratories, Beaumont, TX) after adding 50ng/ml or 500ng/ml of a given cytokine as indicated in text. Tyrode's buffer was added as negative control.

3.3.10 Direct and indirect antigen labeling.

Cells were collected by centrifugation and re-suspended into phosphate-buffered saline (PBS)/2% Bovine Serum (BS). Cells were then stained with FITC or PE conjugated antibodies, or the corresponding isotype controls and incubated for 15 minutes. Cells were washed and analyzed on a FACSCalibur flow cytometer. For indirect labeling, after labeling cells with a primary antibody, cells were stained with the FITC or PE conjugated secondary antibodies. Cells were then analyzed on a FACSCalibur flow cytometer.

3.3.11 Megakaryocyte colony-forming-unit (CFU-MK) assay

CFU-MK assays were preformed according to the manufacturer's instructions (Stemcell Technologies, Inc, Vancouver, Canada). Briefly, UCB CD 34+ cells were cultured in collagen and serum-free MegaCult-C medium supplemented with 10ng/ml IL3, 10ng/ml IL6, 10ng/ml SCF, 50ng/ml TPO (36ST) and with additional cytokines as indicated in the text. After 12 days, cultures were dehydrated, fixed and then immunostained for CD41, a marker of MK differentiation.

3.3.12 TGFβ detection

UCB CD34+ cells were cultured in X VIVO-10 supplemented with 36ST for 10 days. Supernatant was collected and concentrated using Amicon Ultra-15 centrifugal filter units with ultracel-3 membrane (Milipore, Billerica, CA). Culture supernatant was split in half and one fraction was treated with HCl for 10 min followed by neutralization with NaOH/HEPES and the other half was not treated. Detection of TGFβ1 in the treated (i.e. total TGFβ1) and untreated (i.e. activated TGFβ1) were performed using a human TGFβ1 ELISA immunoassay kit (R&D Systems, Minneapolis, MN). Concentrations of total and activated TGFβ1 were determined

against a standard curve. The concentration of latent TGFβ1 in the culture supernatant was calculated by subtracting concentrations of activated TGFβ1 from total TGFβ1.

3.3.13 Statistical analysis

Data is presented as mean ± standard error of the mean and significant differences were determined by analysis of variance (ANOVA).

3.4 RESULTS

3.4.1 Receptor-associated gene expression up-regulated during *in vitro* megakaryocytopoiesis

A genome-wide search to identify all receptors whose ligands might have important functional roles in MK development was performed by using a powerful *in vitro* MK differentiation platform. This involved isolating marrow CD34+/CD38^{lo} cells and culturing the cells for 10 days with a cytokine combination that was previously reported to induce unilineage megakaryocytopoiesis [41]. In our hands, this resulted in 72% ± 5% of cells expressing the CD41 antigen at 10 days of culture and approaches ~90% at 14 days. Using uncultured CD34^{+}/CD38^{lo} cells and culture derived MKs, transcript expression profiles were generated and the profiles were compared to each other to identify differentially expressed genes. A heat map of gene expression levels for replicate samples showed that there was reasonable similarity among the data sets. (Data not shown). Analyses of the data indicated that a total of 3,035 genes significantly changed. Of the differentially expressed transcripts, expression levels for 1,267 increased (i.e. >1.5fold ($p \leq 0.01$) and expression levels for 1,768 decreased (<-1.5 fold ($p \leq 0.01$).

Table 1. Up-regulated plasma membrane receptor genes during megakaryocyte development

*Fold Change	Gene ID	Gene Identifier	Gene Title	Ligand
55.9	ITGB3	M35999	Integrin, beta 3 (platelet glycoprotein IIIa, antigen CD61)	Fibronectin, ADAM15, ADAM23
17.2	ITGA2B	AF098114	Integrin, alpha 2b (platelet glycoprotein IIb of IIb/IIIa complex, antigen CD41)	Fibronectin 1, ICAM 4
16.8	IL21R	NM_021798	Interleukin 21 receptor	IL21
14.5	LRP12	NM_013437	Low density lipoprotein-related protein 12	Orphan receptor
10.4	ITGA6	AV733308	Integrin, alpha 6	ADAM 2, ADAM9, DUSP18
9.0	PTGER3	L27489	Prostaglandin E receptor 3 (subtype EP3)	Prostglandin E2
8.7	CCRL2	AF015524	Chemokine (C-C motif) receptor-like 2	Orphan receptor
8.6	IL9R	NM_002186	Interleukin 9 receptor	IL9
7.8	ADAM10	AU135154	ADAM metallopeptidase domain 10	Orphan receptor
7.2	ITGB5	NM_002213	Integrin, beta 5	ADAM9
7.1	F2R	NM_001992	Coagulation factor II (thrombin) receptor	Thrombin
6.1	HMMR	NM_012485	Hyaluronan-mediated motility receptor (RHAMM)	Hyaluronan synthase 2
5.8	PTGIR	NM_000960	Prostaglandin I2 (prostacyclin) receptor (IP)	Prostacyclin
5.2	SELP	NM_003005	Selectin P (granule membrane protein 140kDa, antigen CD62)	Selectin P ligand, CD24
4.9	SORT1	BE742268	Sortilin 1	Nerve growth factor, beta subunit
4.8	THBD	NM_000361	Thrombomodulin	Platelet factor 4
4.5	CD40	BF664114	CD40 molecule, TNF receptor superfamily member 5	CD40 ligand, lymphotoxin beta (TNF superfamily, member 3)
4.0	CSF2RB	AV756141	Colony stimulating factor 2 receptor, beta, low-affinity (granulocyte-macrophage)	Granulocyte-macrophage colony stimulating factor, IL3, IL5
3.9	C3AR1	U62027	Complement component 3a receptor 1	complement component 3
3.8	ICAM2	NM_000873	Intercellular adhesion molecule 2	ITGAL, ITGB2
3.7	ADRA2A	AF284095	Adrenergic, alpha-2A-, receptor	Dopamine beta-hydroxylase, plasma
3.7	GPR137B	NM_003272	G protein-coupled receptor 137B	Orphan receptor
3.5	LRP8	NM_004631	Low density lipoprotein receptor-related protein 8, apolipoprotein e receptor	Orphan receptor
3.1	HTR2A	NM_000621	5-hydroxytryptamine (serotonin) receptor 2A	Tryptophan hydroxylase 1
3.0	CD63	NM_001780	CD63 molecule	Orphan receptor
2.9	TGFBR2	D50683	transforming growth factor, beta receptor II (70/80kDa)	TGFb
2.8	CD47	Z25521	CD47 molecule	Thrombospondin I & II
2.7	IL6ST	AL049265	Interleukin 6 signal transducer (gp130, oncostatin M receptor)	IL6, leukemia inhibitory factor, oncostatin M, ciliary neurotrophic factor, IL11, IL6, NP (ortholog of mouse neuropoietin)
2.7	ACVR1	NM_001105	Activin A receptor, type I	Bone morphogenetic protein 6 & 7
2.7	ITGB1	BG500301	integrin , beta 1	ADAM 12, 15, 17, 2, 9
2.5	IL4R	NM_000418	Interleukin 4 receptor	IL4, IL13
2.2	TSPAN4	AF054841	Tetraspanin 4	Orphan receptor
2.1	CD55	BC001288	CD55 molecule, decay accelerating factor for complement (Cromer blood group)	CD97
2.0	ADIPOR2	NM_024551	Adiponectin receptor 2	Adiponectin, C1Q and collagen domain containing
1.9	IL10RB	BC001903	Interleukin 10 receptor, beta	IL10
1.8	SEMA4D	NM_006378	Sema domain, immunoglobulin domain (Ig), transmembrane domain (TM) and short cytoplasmic domain, (semaphorin) 4D	Plexin B1
1.7	PTPRA	AL121905	protein tyrosine phosphatase, receptor type, A	Orphan receptor
1.6	TSPAN31	NM_005981	Tetraspanin 31	Orphan receptor
1.6	TFG	NM_006070	TRK-fused gene	Orphan receptor
1.6	ATRN	AL132773	attractin	Agouti signaling protein

*Fold-change from 3 independent experiments; p-value≤0.01

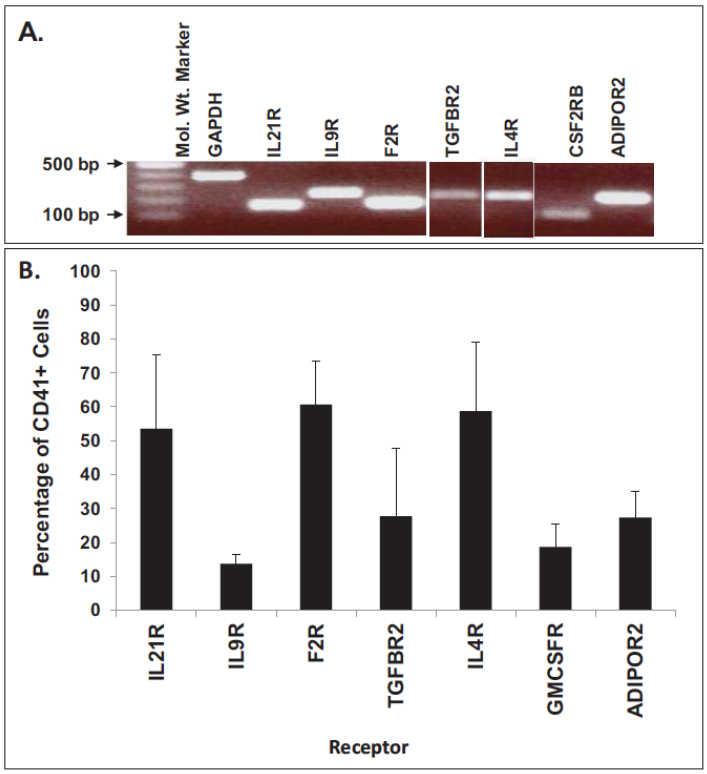

Figure 3.1 RNA and protein expression for each of 7 receptors is confirmed in MKs.

Umbilical cord blood CD34+ cells were cultured with interleukin IL3, IL6, SCF, and TPO. After 10 days of culture, the CD41+ cells were isolated by flow cytometry. A) RT-PCR confirmation of receptor expression in CD41+ cells. B) Percentages of CD41+ cells that express each receptor as measured by flow cytometry. Data are shown as mean±SEM and are representative of three independent experiments and from three biological samples.

To identify potential paracrine/autocrine signaling systems involved in MK development, the Human Plasma Membrane Receptome database (http://receptome.stanford.edu) was used to interrogate genes contained within the microarray dataset that are classified as membrane receptome genes. Investigation of the transcriptome database against a liganded receptome revealed that there were 40 ligand-receptor genes whose expression was up-regulated (Table 1) and 37 ligand-receptor genes whose expression was down-regulated ligand (Table 2). The analyses also revealed that among the 40 receptor genes whose expression were up-regulated

were 10 classified as orphan receptor genes and among 37 genes whose expression waa down-regulated there were 11 orphan receptors. The receptors were then surveyed against a defined set of "training genes" known to be specifically critical for the development and function of megakaryocytes and platelets (i.e. megakaryome, 519 genes). Of the 40 up-regulated genes, 11 transcripts were found to be common to the megakaryome dataset. The common genes whose expression was up-regulated included ADAM10, CD55, CD63, F2R, ICAM2, IL6ST, ITGA2B, ITGB1, ITGB3, PTGIR, and SELP. Since it is unlikely that genes down-regulated during MK development are involved in the function of MKs and platelets, it was not surprising that only 1 gene of the 37 down-regulated receptor genes, ITGA2, was also found in the megakaryome dataset.

To validate the robustness of the microarray dataset, a sub-set of 7 genes from the list of 40 up-regulated ligand-receptor pairs were chosen for further examination. These 7 receptor genes were chosen because their ligands were commercially available. Of the 7 receptor genes, only the coagulation factor II (thrombin) receptor (F2R) was common to both the megakaryome and Human Plasma Membrane Receptome. The remaining 6 genes, IL21R, IL9R, CSF2RB, ADIPOR2, TGFBR2, and IL4R were not found in the megakaryome database.

RNA and protein expression levels in MKs were confirmed for each of the 7 genes. RT-PCR was used to verify RNA levels in culture derived MKs (Figure 3.1A) and flow cytometry was used to examine protein levels. Greater than 50% of culture derived CD41+ cells expressed IL21R, F2R, and IL4R (Figure 3.1B). Receptors, IL9R, TGFBR2, CSF2RB, and ADIPOR2 were expressed on 14%, 28%, 19% and 27% of MKs, respectively (Figure 3.1B).

Table 2. Plasma membrane receptor genes down-regulated during megakaryocyte development.

*Fold Change	Gene ID	Gene Identifier	Gene Title	Ligand
0.63	ADAM22	AW242701	Transcribed locus	Leucin-rich, glioma inactivated 1 (LGI1)
0.62	TYRO3	D50479	TYRO3 protein tyrosine kinase	growth arrest-specific 6 (GAS6), Protein S, alpha
0.61	GPR35	AF089087	G protein-coupled receptor 35	kynurenic acid
0.57	EDA2R	NM_021783	Ectodysplasin A2 receptor	Ectodysplasin A
0.54	GPR56	AL554008	G protein-coupled receptor 56	Transglutaminase 2 (TGM2)
0.50	LILRB3	NM_024318	Leukocyte immunoglobulin-like receptor, subfamily B (with TM and ITIM domains), member 3	Orphan Receptor
0.46	EMR2	NM_013447	Egf-like module containing, mucin-like, hormone receptor-like 2	Orphan Receptor
0.45	NOTCH4	AI743713	Notch homolog 4 (Drosophila)	Delta-like 4 (DLL4)
0.45	CNTN1	U07820	Contactin 1	Contactin-associated protein 1 (CNTNAP1), protein-tyrosine phosphatase zeta precursor (PTPRZ1)
0.41	FLT1	AA058828	Fms-related tyrosine kinase 1 (vascular endothelial growth factor/vascular permeability factor receptor)	Vascular endothelial growth factor (VEGF)
0.39	IL18R1	NM_003855	Interleukin 18 receptor 1	IL18
0.39	FGFR1	M60485	Fibroblast growth factor receptor 1	FGF1, FGF3, FGF4
0.38	CD53	NM_000560	CD53 molecule	Orphan Receptor
0.36	LPHN1	NM_024679	latrophilin 1	SH3 and multiple ankyrin repeate domains 1 (SHANK1)
0.29	SELL	NM_000655	Selectin L	CD34-molecule (CD34), complement factor H (CFH), ppodocalyxin-like 2 (PODXL2)
0.28	ITGA9	NM_002207	Integrin, alpha 9	ADAM12, ADAM15
0.26	PTGER2	NM_000956	Prostaglandin E receptor 2 (subtype EP2), 53kDa	Prostglandin E2
0.21	CD97	NM_001784	Leucocyte antigen CD97	Decay-accelerating factor for complement (CD55_
0.21	PVRL2	AI520949	Poliovirus receptor-related 2 (herpesvirus entry mediator B)	Orphan Receptor
0.21	EPHB4	NM_004444	EPH receptor B4	Ephrin B2 (EFNB2), ephrin B1 (EFNB1)
0.20	TSPAN32	AF176071	Tetraspanin 32	Orphan Receptor
0.16	TSPAN18	AL565381	Transcribed locus	Orphan Receptor
0.16	ITGA2	N95414	Integrin, alpha 2 (CD49B, alpha 2 subunit of VLA-2 receptor)	CHAD, COL1A2, COL2A1
0.15	IL17RA	BF939473	Hypothetical protein LOC150166	DUSP18, FN1
0.12	GPRC5B	NM_016235	G protein-coupled receptor, family C, group 5, member B	Orphan Receptor
0.11	TSPAN14	BF025955	Tetraspanin 14	Orphan Receptor
0.10	TNFRSF10D	AI738556	Tumor necrosis factor receptor superfamily, member 10d, decoy with truncated death domain	TNF, Oligodendrocyte myelin glycoprotein (OMG)
0.10	ROBO4	AA156022	Roundabout homolog 4, magic roundabout (Drosophila)	SLIT, drosophila, homolog of, 2 (SLIT2)
0.09	GPR160	BC000181	G protein-coupled receptor 160	Orphan Receptor
0.07	CD44	AV700298	CD44 molecule (Indian blood group)	hyaluronan synthase 2 (HAS2)
0.04	TSPAN5	AI928507	Tetraspanin 5	Orphan Receptor
0.03	GPR161	AI743151	G protein-coupled receptor 161	Dopamine beta-hydroxylase, plasma (DBH)
0.02	ITGA8	BF939224	Integrin, alpha 8	Nephronectin (NPNT)
0.02	IFNGR1	AI458949	Interferon gamma receptor 1	Interferon-gamma (IFNG)
0.02	GPR98	AW339783	G protein-coupled receptor 98	Orphan Receptor
0.003	AGR2	AI922323	Anterior gradient homolog 2 (Xenopus laevis)	Prod 1 in the salamander model
0.002	ROR1	AK000776	CDNA FLJ20769 fis, clone COL06674	Orphan Receptor

*Fold-change from 3 independent experiments; p-value≤0.01

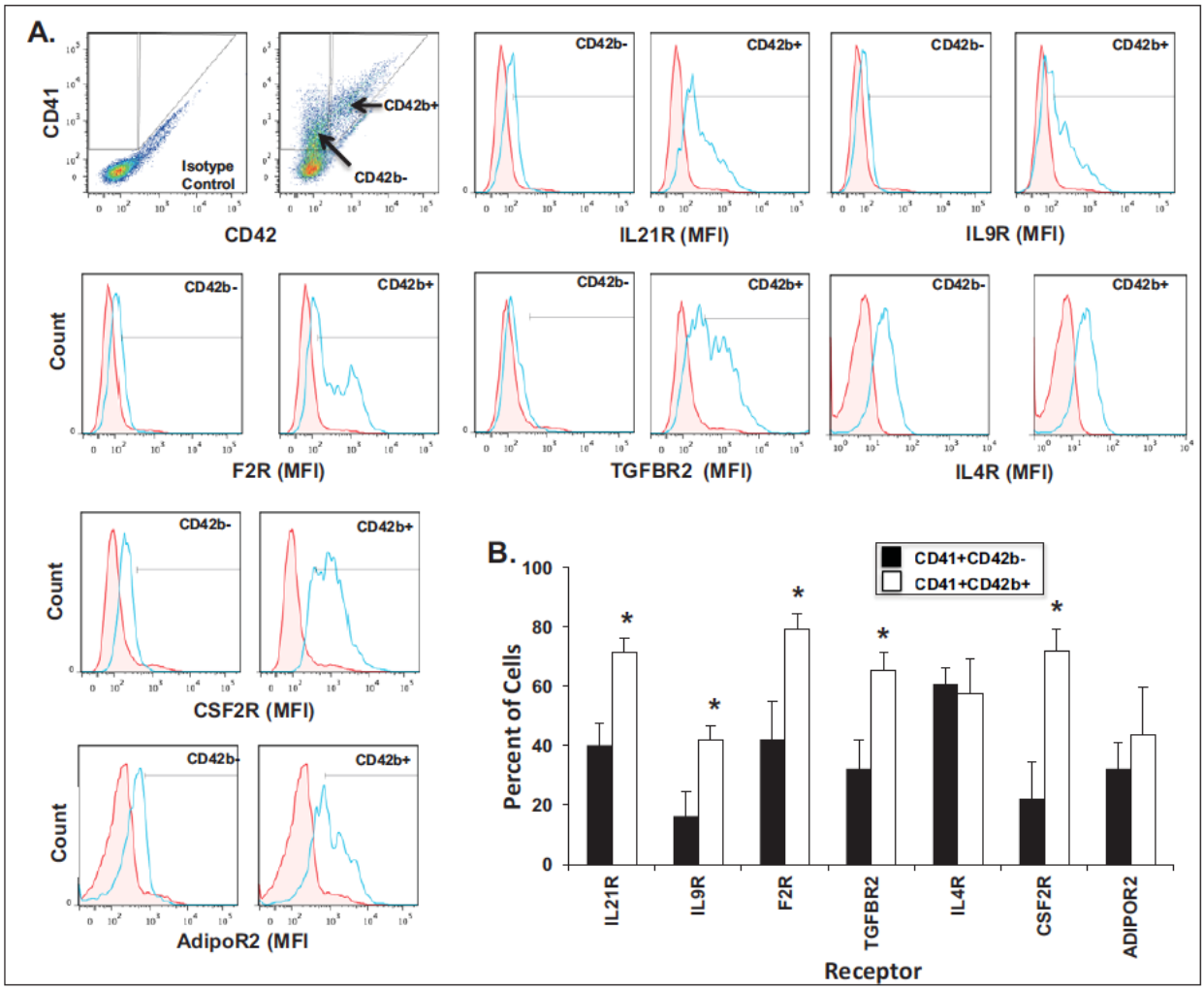

Figure 3.2 Protein expression for each of 7 receptors increases as MKs mature.

Culture derived MKs were isolated and immunostained for CD41, CD42b and for each of the indicated receptors. A) Dot plot analysis of CD42 and CD41 expression on culture-derived MKs was used to define gates for the subpopulations, CD41+/CD42b+ and CD41+/CD42b-. Representative single parameter histogram profiles for gated CD41+ CD42b- cells or CD41+CD42b+ cells were generated depicting the mean fluorescent intensity (MFI) for each receptor relative to an isotype control (red=isotype control; blue=receptor). B) The percent of CD41+ CD42b- cells and CD41+CD42b+ cells that express the indicated receptor as measured by flow cytometry. Values are mean SEM and are representative of three independent experiments and from three biological samples. *$p<0.05$

To further investigate receptor expression during MK maturation, we compared receptor expression on a subpopulation of CD41+CD42b- MKs to a more mature subset of MKs defined

as CD41+ CD42b+ (Figure 3.2). Histogram plots revealed that the fluorescence intensity for each of the 7 receptors was greater on CD41+CD42b+ cells than on CD41+CD42b+ cells (Figure 3.2A). Consequently, the percentage of cells expressing each of the 7 receptors was significantly higher on CD41+ CD42b+ cells than on CD41+ CD42b- cells (Figure 3.2A & B).

3.4.2 Proliferation and differentiation responses to each receptor's cognate ligand

Functional roles for each of the 7 receptors during megakaryocytopoiesis were probed by evaluating the effects of their cognate ligands on *in vitro* MK development. The ligands IL21, IL9, Thrombin, TGFβ, IL4, adiponectin, and GM-CSF were used to test whether the plasma membrane receptors IL21R, IL9R, F2R, TGFβR2, IL4R, ADIPOR2, and CSF2RB facilitated MK development, respectively. This was accomplished by initiating cultures of UCB CD34+ cells with a MK induction base media containing the cytokine combination of 36ST (i.e. control) plus one of the following cytokines: IL21, IL9, Thrombin, TGFβ, IL4, adiponectin, or GM-CSF. After 10 days of culture. Results showed that relative to control cultures (i.e. 36ST only) the proliferation of UCB CD34+ cells was significantly increased with the addition of GM-CSF, and inhibited with TGFβ and adiponectin (**Figure 3.3**A). The remaining cytokines did not have an apparent effect on proliferation (**Figure 3.3**A).

Since gene expression for each of the 7 receptors increased as cells underwent MK development, we rationalized that addition of their matched-ligand might have a greater impact on culture outcome if added late in the cultures (i.e. at day 7 of culture) rather than at the time that the cultures were initiated. To execute these experiments, UCB CD34+ cells were cultured for 7 days with 36ST prior to the addition of each individual test cytokine and cultured for an additional 7 days. The results now showed that IL9 had a positive impact on proliferation and

even though not significant GM-CSF continued to promote cell proliferation (**Figure 3.3**B). TGFβ strongly inhibited cell proliferation independent of whether it was added at day 0 or day 7. (**Figure 3.3**B). Decreased cellular outputs were also apparent in the presence of adiponectin and IL4, however, neither reached statistical significance.

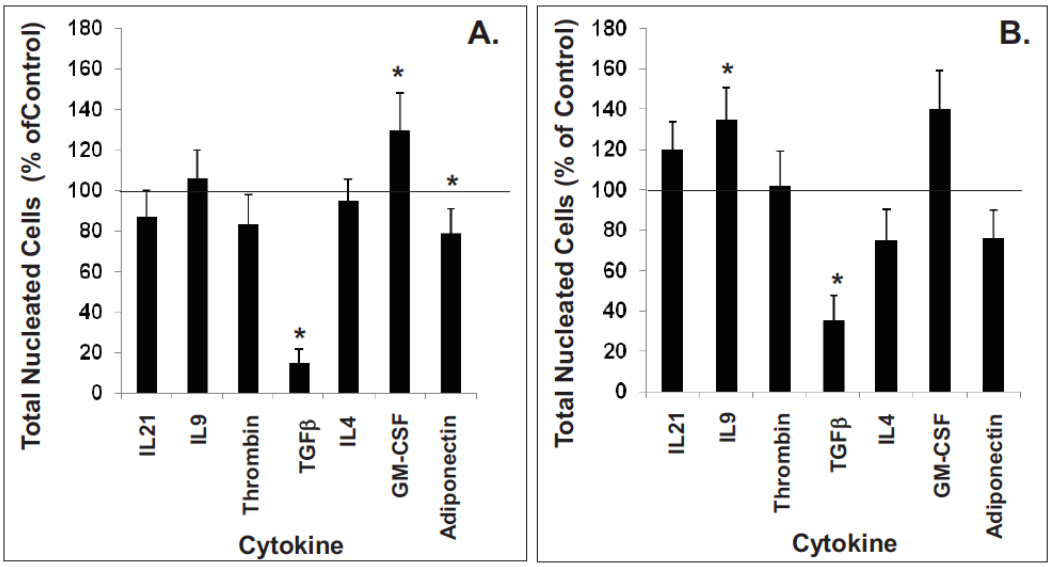

Figure 3.3 Proliferation responses.

Umbilical cord blood CD34+ cells were cultured for10 days with IL3, IL6, SCF, TPO (36ST) (i.e. control). A) 36ST was added at day 0 along with one of the indicated cytokines; B) 36ST was added at day 0 and one of the indicated cytokines was added at day 7. After 10 days of culture, the number of total nucleated cells was counted. The proliferation response is expressed as a percent of the control group. The line in each graph represents a proliferation response of 100% (i.e. control response). Data are shown as mean±SEM in triplicate culture and are representative of three independent experiments from three biological samples. *$p<0.05$.

The impact that each of the 7 cytokines had on the differentiation response of UCB CD34+ cells as the cells were induced along the MK lineage was measured by monitoring the expression level of the CD41 antigen as well as a feature unique to megakaryocytopoiesis, polyploidization. When one of the 7 cytokines in question was added at the time UCB CD34+ cultures were initiated with base medium containing 36ST, the percent of cells expressing CD41 at day 10 of

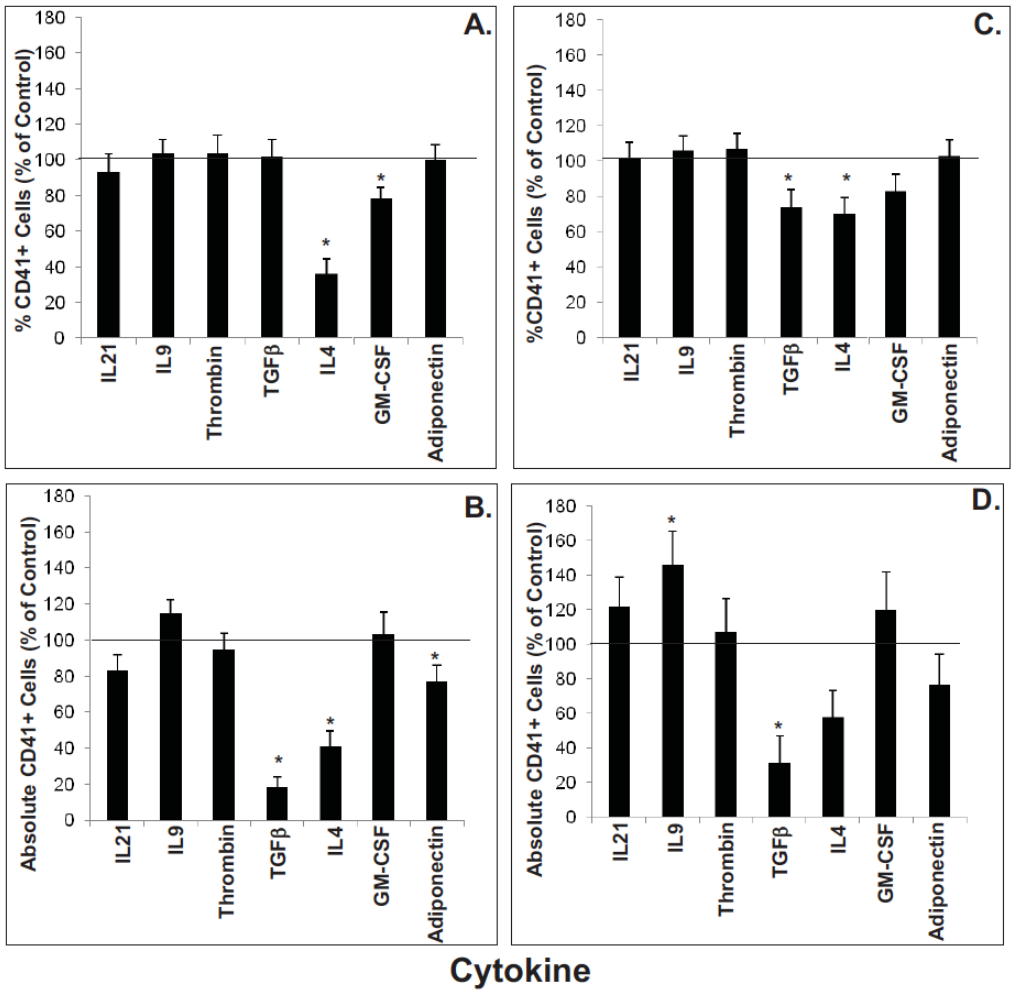

Figure 3.4 Differentiation responses.

A & B) Umbilical cord blood CD34+ cell cultures were initiated with IL3, IL6, SCF, TPO (36ST) (i.e. control) along with one of the indicated cytokines. After 10 days of culture, the percent of CD 41+ cells in culture was measured by flow cytometry. C & D) Umbilical cord blood CD34+ cell cultures were initiated with 36ST. After 7 days in culture, one of the indicated cytokines was added. A-D), the percent of CD41+ cells in culture was measured by flow cytometry. The percent and absolute number of cells expressing CD41+ is normalized to the control group. Data are shown as mean±SEM in triplicate culture and are representative of three independent experiments and from three biological samples. *$p<0.05$.

culture was similar to control cultures except when IL4, and GM-CSF were present in the cultures (**Figure 3.4**A). The absolute counts showed that fewer total CD41+ cells were produced relative to control cultures in the presence of TGFβ, IL4, and adiponectin (**Figure 3.4**B). The

results also showed that when ligand addition occurred 7 days after culture initiation with 36ST the percent of cells expressing CD41 was similar to the control except in the presence of TGFβ and IL4 (**Figure 3.4**C). While absolute counts indicated that there were significantly greater numbers of CD41+ cells with IL9 when present in cultures and fewer total CD41+ cells with TGFβ when present in cultures relative to control cultures (**Figure 3.4**D). The results of ploidy analyses indicated that no significant changes in polyploidization was observed when each of the 7 cytokines were added at the time that UCB CD34+ cultures were initiated with 36ST (data not shown).

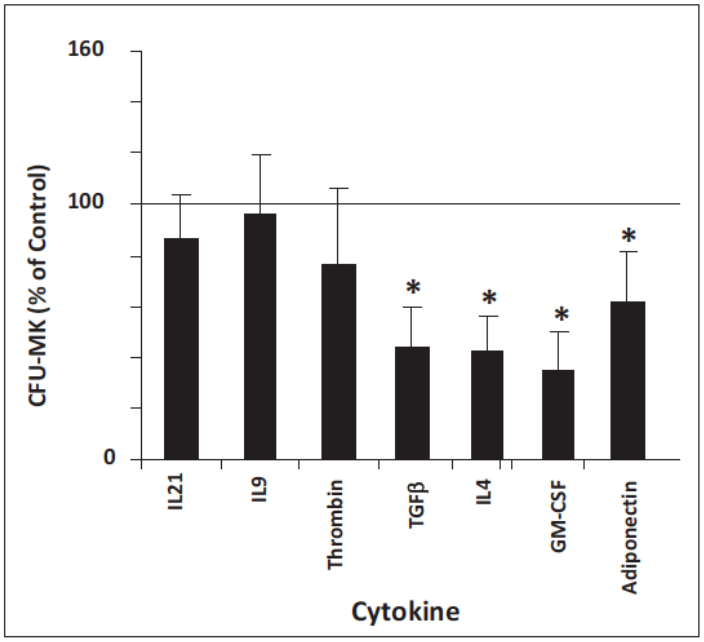

Figure 3.5 Megakaryocyte colony-forming-unit (MK-CFU) formation.

Cord Blood (UCB) CD34+ cells were cultured for 12 days with interleukin (IL)- 3, IL6, SCF, TPO (36ST) plus one of the indicated cytokines in collagen containing media. CD34+ cells cultured with only 36ST were designated as controls. The number of colony-forming unit megakaryocytes (CFU-MK) were counted as described in Materials and Methods and normalized with control group. Data are shown as mean±SEM in duplicated culture and are representative of three independent experiments and from three biological samples. *$p<0.05$.

The effect of each cytokine on the formation of CFU-MKs is shown in **Figure 3.5**. Significant reductions in colony formation by 56%, 57%, 31% and 38% relative to control cultures were seen with TGFβ, IL4, GM-CSF and adiponectin, respectively. The cytokines, IL21, IL9, and thrombin did not cause any significant change in CFU-MK formation.

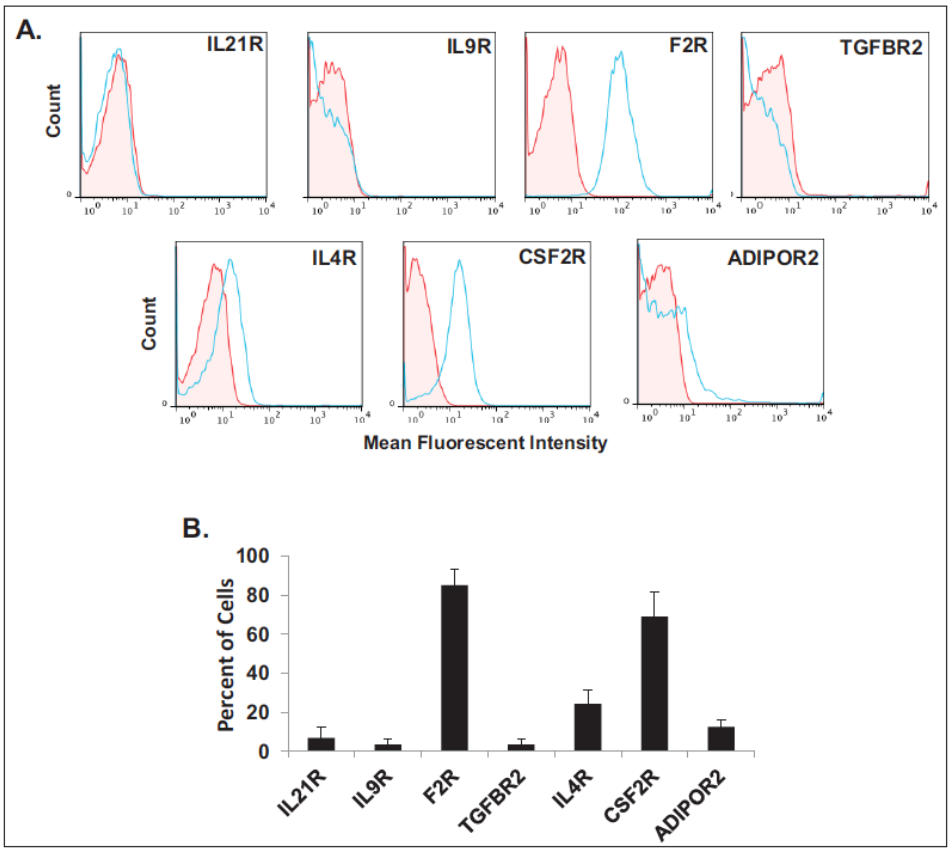

Figure 3.6 Platelet receptor expression.
Fresh whole blood platelets were isolated and immunostained with antibodies to CD41 or CD61 and for the indicated receptors. A) Representative single parameter histogram profiles for CD41+ or CD61+ gated platelet populations were generated depicting the mean fluorescent intensity (MFI) for each receptor relative to an isotype control (red=isotype control; blue=receptor). B) The percent of platelets that express the indicated receptor as measured by flow cytometry. n=4

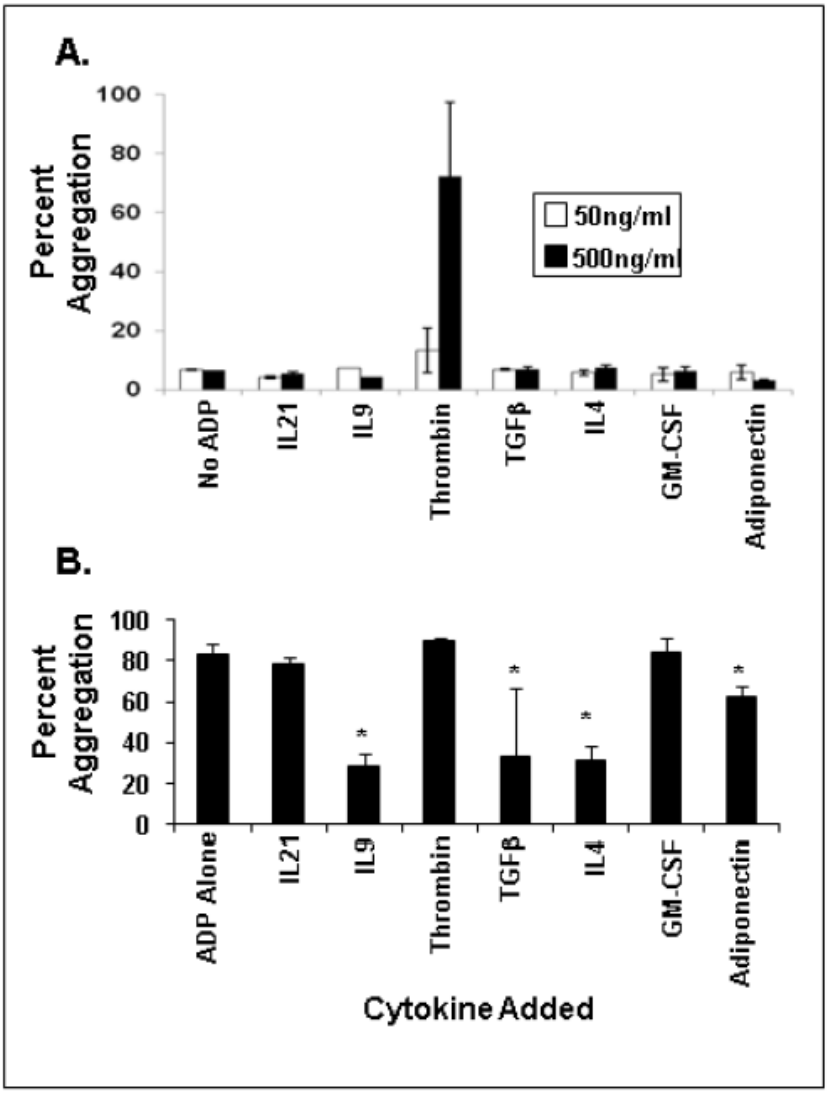

Figure 3.7 Platelet aggregation responses.
Fresh whole blood platelets were isolated and aggregation of platelets in response to the paired cytokines for each of the 7 receptors was measured. A) Maximum percent platelet aggregation in response to 50ng/ml or 500ng/ml for each of the indicated cytokines. Data is shown as mean SEM; n=2. B) Platelets were pre-incubated with 500 ng/ml of the indicated cytokine for 5 min. After which 20 M of ADP was added and the percent aggregation was measured using an aggregometer. Data is shown as mean SEM; n=3.

3.4.3 Receptor expression on platelets

As the terminal differentiation of MKs culminates in the formation of platelets, we examined the expression level of the 7 receptors in platelets. Flow cytometry revealed that 92±5%, 68±21%, and 68±5% of platelets expressed F2R, CSF2RB, and ADIPOR2 (mean± SEM),

respectively (**Figure 3.6**A). IL4R, IL21R, IL9R and TGFBR2 were expressed on only 4.3±1.5%, 1.3±0.9%, 1.3±0.9%, and 0.7+1.2% of platelets, respectively. Even though receptors F2R, CSF2RB and ADIPOR2 were highly expressed on platelets. Platelet aggregation studies showed that only thrombin induced platelet aggregation (**Figure 3.7**A). However, when platelets were pre-incubated with 500 ng/ml of one of the 7 cytokines for 5 minutes, prior to the addition of the platelet agonist, ADP. ADP-induced platelet aggregation was significantly decreased by 28%±7%, 34%±31%, 32%±7% and 62%±5% of aggregation when IL9, TGFβ1, IL4 or adiponectin were pre-incubated with platelets (**Figure 3.7**B).

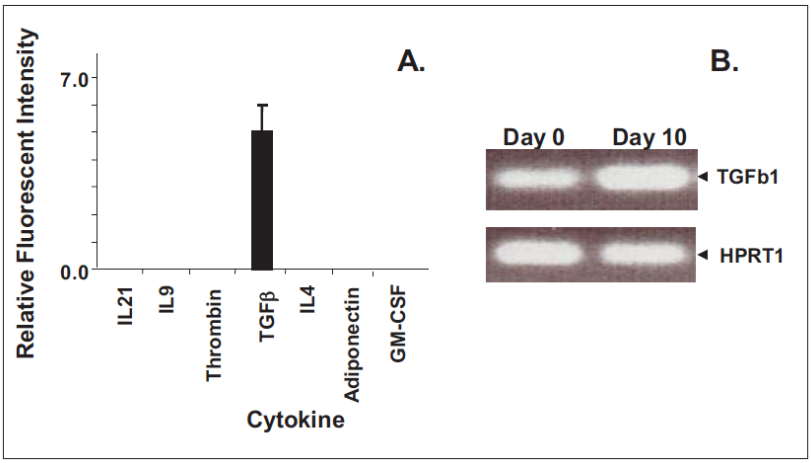

Figure 3.8 TGFβ1 is the only auto-expressed matched-ligand for 7 receptors that were identified as being up-regulated during MK development.

The same microarrays used to identify the up-regulation of IL21R, IL9R, F2R, TGFBR2, IL4R, ADIPOR2, and CSF2RB during MK development were also searched for the expression of their matched-ligands. A) Fold change in relative fluorescent intensities in marrow CD34+/CD38lo cells relative to culture derived MKs. Positive fold changes indicate higher RNA expression levels by culture derived MKs than day 0 CD34+/CD38lo cells. Data are shown as mean±SD from three independent experiments. B) Umbilical cord blood CD34+ cells (Day 0) were cultured with IL 3, IL6, SCF,TPO. After 10 days of culture, CD41+ cells were isolated by flow cytometry. RNA was isolated, semi-quantitative RT-PCR was performed and the PCR products are shown on a 1% agarose gel.

3.4.4 Auto-Expression of Cognate Ligands

Since autocrine signaling can regulate stem cell development, the microarray data were analyzed to determine whether transcripts for cytokines to each of the 7 receptors IL21R, IL9R, F2R, TGFBR2, IL4R, ADIPOR2, and CSF2RB were differentially expressed between uncultured $CD34^{+}/CD38^{lo}$ cells and culture derived MKs. We found that only the transcript for the cytokine TGFβ increased in expression level. This finding was confirmed by semi-quantitative RT-PCR of culture-derived MKs (**Figure 3.8**). To determine whether this translated into a secretion of TGFβ by developing MKs, we examined culture supernatants and found TGFβ levels of 2,228±1,599 pg/ml of media (n=5). Further analysis indicated that the majority of the secreted TGFβ was in the latent form.

3.5 DISCUSSION

A microarray analysis identified a list of 40 molecules that constitutes a developing MK receptome (Table 1). This list is composed of plasma membrane receptor genes that are significantly up-regulated as $CD34^{+}/CD38^{lo}$ cells are induced to become MKs. Of 7 of the 40 differentially expressed transcripts that are selected to validate the robustness of the dataset, protein expression levels for all 7 are observed in MKs. Furthermore, the robustness of the dataset is illustrated by our findings that six of 7 matched ligand-receptor axes, IL9/IL9R, thrombin/F2R, TGFβ/TGFBR2, IL4/IL4R, GM-CSF/CSF2RB, and adiponectin/ADIPOR2, have significant biological effects on the MK lineage. Of the 7 cytokine receptors expressed by MKs, F2R, and CSF2RB remained present on platelets, but IL21R, IL9R, TGFBR2 and IL4R were absent or negligibly detected. Of the 7 matched-receptor ligands, the IL21 cytokine was the only one we were unable to detect a biological effect on MK development. However, because assays

were limiting in this study, this does not preclude a role for the IL21/IL21R ligand-receptor axis in the biology of MKs/platelets.

This is the first study to show that MK colony formation is inhibited significantly by adiponectin ($p=0.037$). Thus, indicating that levels of adiponectin are relevant for regulating megakaryocytopoiesis. Adiponectin is a well-documented regulator of a number of metabolic processes [65], it is expressed in adult bone marrow [66], and in 2007 was identified as a novel hematopoietic stem cell growth factor [67]. Adiponectin levels inversely correlate with body fat content in adults [68, 69], and in individuals with hematological disorders [70, 71]. Adiponectin suppresses bone marrow granulocyte/macrophage colony formation [72], and is secreted by adipocytes as well as by a number of other cell types [72-77]. Adipocytes are the most abundant stromal cells in adult bone marrow [78] and are a production site for TNFα[79] and TGFβ [80], which inhibit both fat formation and MK maturation. Using a human cytokine antibody array, it was also recently shown that adiponectin is among a group of cytokines with the highest levels of detection in platelet lysates [81]. Based on our findings along with findings from other investigators, it is intriguing to speculate that MK progenitor production may be regulated in part by adiponectin levels. Given the inverse correlation of body fat content to adiponectin levels and our finding that adiponectin inhibits CFU-GM, the prediction is that the production of MK progenitors will decrease as adiponectin levels increase or as body fat content decreases. This prediction is partially supported by the observation that obese females have significantly elevated platelet counts compared with normal-weight females (30). However, a key question that remains to be addressed is what causes adiponectin levels to decrease as fat content increases when adipocytes are the major source of adiponectin? In addition, our observation that adiponectin inhibits ADP-induced platelet aggregation supports a role for adiponectin in

modulating platelet function. This observation is in agreement with a previous report that indicates that high concentration of adiponectin (>25ug/ml) diminishes epinephrine- and ADP-induced platelet aggregation (27).

Our finding that TGFβ1 strongly inhibits MK development is in agreement with work by other investigators, [20, 82, 83]. An examination of our microarray dataset for autocrine expression of cognate ligands to the 7 selected receptors only showed that transcripts for the TGFβ cytokine were up-regulated. This was confirmed by the finding that there was an autocrine secretion of TGFβ in the supernatant of MK cultures. TGFβ when exogenously added to cultures inhibited the proliferation of MK progenitors. However, autocrine TGFβ had apparently no inhibitory effect on *in vitro* megakaryocytopoiesis because the autocrine cytokine was predominantly in a latent form. The observation that there is an autocrine secretion of latent TGFβ into culture supernatant is important. Especially when considering the design of stem cell culture systems with feeder cells, such as endothelial and/or stromal cells, to support an *in vitro* MK production. As feeder cells produce TSP-1, MMP-9 and MMP-2, which are known to cleave latent TGFβ [84, 85]. Consequently, a bioreactor design with such a co-culture design may require an addition of neutralizing antibodies and/or antagonists to TGFβ1 to enhance MK development.

This is the first report that CSFR2B is expressed on MKs and platelets. CSFR2B is the common beta chain for not only the GM-CSF receptor, but also for the IL-3 and IL5 receptors. [86] Although other studies have reported that GM-CSF modestly stimulates CFU-MK formation [87], in our study GM-CSF inhibited MK colony formation and MK differentiation. This contradiction in findings may be due to the concentration of GM-CSF. As Chen et al, indicate that low concentrations of GM-CSF stimulate MK colony formation and high doses are

inhibitory [88]. On the other hand, we suspect that the high proliferative responses (i.e. increased TNC counts) in the presence of GM-CSF even while CFU-MK progenitor growth is inhibited is most likely due to GM-CSF supporting the growth of other hematopoietic cell lineages such as granulocytes and monocytes [89]. As noted by D'Atri LP *et al* the inhibitory effect of GM-CSF on CD41+ cells is a result of a switch of CD34+ cells differentiation towards the monocytic lineage [8]. The finding that CSFR2B is also expressed on platelets suggests that GM-CSF might have a biological role in modulating platelet function. However, despite the presence of CSF2RB on platelets and in agreement with the findings of other investigators [90] GM-CSF alone did not induce platelet aggregation.

Not surprisingly, different proliferation and differentiation responses were noted dependent upon the timing of when some of the 7 cytokines were individually added to UCB CD34+ cultures that were initiated with base medium containing 36ST. This was especially evident when comparing the proliferation response of cells supplemented with IL9 at day 0 versus day 7 of culture. When IL9 was added at day 7 of culture, IL9 significantly increased the proliferative response of cells (Fig. 2B). However, IL9 had no apparent effect on the number of TNCs produced when added at the time that cultures were initiated (Fig. 2A). IL9 stimulatory effects on MK development are in agreement with a previous report from the literature [16].

These studies validate that differentially expressed plasma-membrane receptors identified by our microarray analyses of developing MKs have functional roles in megakaryocytopoiesis and platelet biology. Thus, suggesting that there is a strong likelihood that the remaining 33 of the 40 up-regulated plasma membrane-localized receptors have important biological roles in the function and/or development of MKs and platelets (Table 1). Among the remaining 33 genes are ligand-receptor pairs that have been implicated in MK development, but receptor expression has

not been definitively reported in MKs. There are also orphan receptors on this that could help to identify new ligands that participate in megakaryocytopoiesis (Table 1). The creation of a developing MK receptome provides an opportunity for users to identify functional roles for previously uncharacterized matched receptor-ligand systems that integrate a multiplicity of environmental cues that are critical for MK development and platelet biology. Moreover, this work provides a foundation for subsequent studies to characterize the role of the plasma-membrane-localized receptors that were found to be down-regulated as stem cells were induced to differentiate (Table 2).

Chapter 4 Development of 3D microsystem to mimic bone marrow niche of thrombopoiesis

4.1 Abstract

Bone marrow is the key location for megakaryocytes (MKs) maturation and platelets generation. Complicated hematopoietic niches for thrombopoiesis contain physical support, soluble factors and cell-mediated interactions. Traditional 2D liquid culture system only provides part of the extracellular cues, e.g. proper soluble factor combination, pH, but not the others, causing the difficulties to produce mature MKs and large scale of functional platelets *in vitro*. This chapter describes a 3-D culture system to mimic bone marrow hematopoietic niche for thrombopoiesis. This biomimetic microdevice contains a microvessel network, extracellular matrix and perivascular stromal cells. Lithography technology has been used to develop the 3-D collagen based microchannel. Specialized microchannel geometry allows a spatial distribution of flow velocity in one device, which helps potential study of the endothelium change under precisely controlled shear stress. Endothelial cells were seeded into microchannel, while two different bone marrow stromal cells were mixed with collagen and cultured in the perivascular area. This biomimetic microdevice could be not only a platform to study thrombopoiesis, but also broader applications in other vascular systems.

4.2 Introduction

Bone marrow hematopoietic niche provide physical support, soluble factors and cell-mediated interactions to regulate the function of hematopoietic cells. Usually bone marrow hematopoietic niches are divided into two different niches: endosteal niche, which is populated by osteoblast,

and vascular niche, which is populated by endothelial cells and perivascular cells[91]. However, the two niche are sometimes located closed to each other and it is difficult distinct one from the other. Locations of MKs in bone marrow change during MK development. HSCs reside close to osteoblasts. During the differentiation of MKs, MK progenitors and immature MKs migrate from endosteal niche to vascular niches. The last maturation of MKs and shedding of platelets occur in the bone marrow sinus. For thrombopoiesis study, vascular niche is the main location for generating platelets. The components of vascular niche includes sinusoid, cells in the perivascular space and supportive extracellular matrix. Our lab reported *in vitro* microvessels for the study of angiogenesis and thrombosis [92]. In this chapter, we would adapt the microvessel and develop a 3-D microdevice to mimic the bone marrow vascular niche.

4.3 Materials and Methods

4.3.1 Antibodies

Rabbit polyclonal CD31 antibody was purchased from Abcam (Cambridge, MA). Hoechst 33342 was purchased from Invitrogen (Grand Island, NY).

4.3.2 Culture of bone marrow stromal cell lines

Bone marrow stromal cell lines GFP-HS27A and GFP-HS5, that were gift from Torok-Storb lab in Fred Hutchinson Cancer Research Center, were generated by infecting HS27A and HS5 with a Toledo strain cytomegalovirus (CMV) containing the gene for green fluorescent protein (GFP) under the control of elongation factor-1 promoter [93]. HS-27a and HS-5 were grown in RPMI 1640 medium (Gibco, Carlsbad, CA) supplemented with L-glutamine (0.4 mg/mL), sodium pyruvate (1 nmol/L), and 10% fetal calf serum at 37^{o}C in a 5% CO_2 humidified chamber.

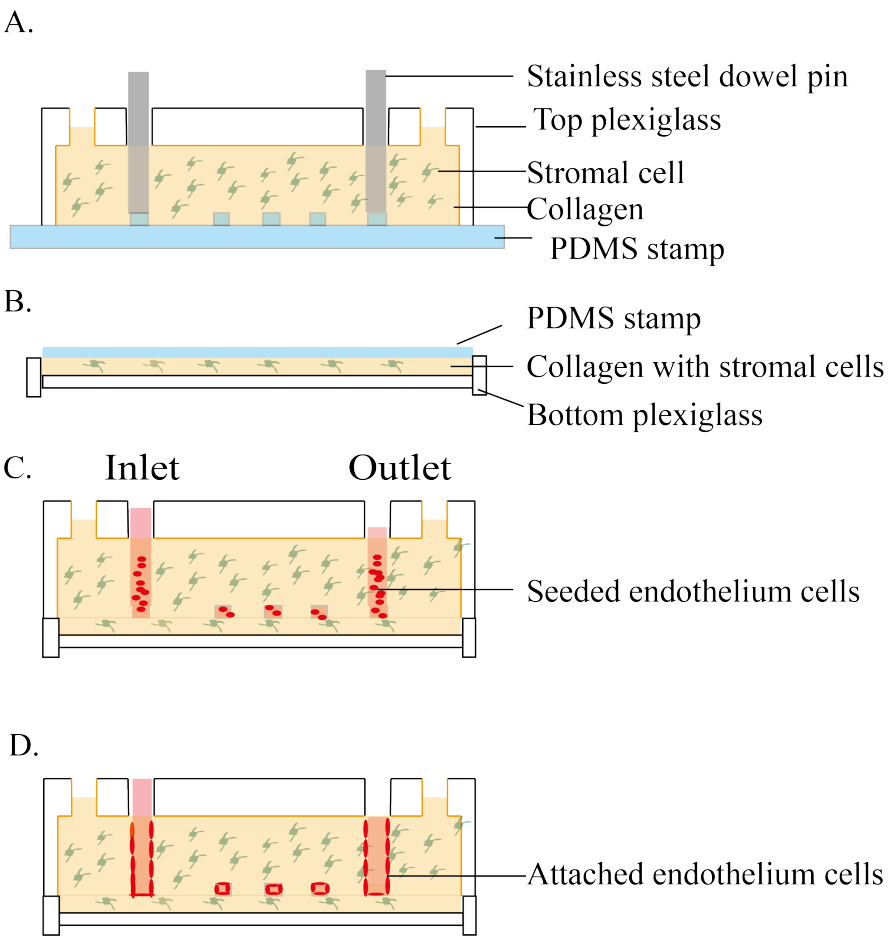

Figure 4.1 Schematic representation for a 3-D bone marrow niche microdevice fabrication.

(A) Top jig was assembled with a PDMS stamp containing the microvessel feather. Two stainless steel dowel pins were used to block collagen diffusion and create space for inlet and outlet. Type 1 collagen mixed with stromal cells was injected into the assembled top jig. (B) Bottom jig was assembled with a flat PDMS stamp. A thin layer of collagen with stromal cells was formed. (C) Top and bottom jigs were assembled together. Stainless pins were removed and HUVECs were seeded from inlet. (D) HUVECs attach to the collagen-based microchannel.

4.3.3 Culture of human umbilical vein endothelial cells (HUVECs)

HUVECs (Lonza) were cultured in endothelial cell growth media (EGM, Lonza) at 37^{o}C in a 5%

CO_2 humidified chamber. Passages 5 to 6 of HUVECs were used in experiments.

4.3.4 Type 1 collagen gel preparation

Type I collagen was harvested from frozen rat tail as described in [92]. Briefly, collagen was extracted from rat tails, rinsed with ethanol to remove endotoxin and dissolved in 0.1% acetic acid. After at least 48 hours of solubilization, collagen was centrifuged at at 4°C, RPM 8000, for 90 minutes. The supernatant was collected and froze in -20°C. The frozen collagen was lyophilized and resuspended in 0.1% acetic acid at a stock concentration of 15mg/ml. 7.5 mg/ml of collagen was prepared on ice right before the injection into 3D microdevice with EGM, 10X M199 (Lonza) and 1N NaOH.

4.3.5 Design and fabrication for 3D biomimic microdevice

Fabrication of the 3D biomimetic microdevice was shown in Figure 4.1. The microdevice contains two plexiglass jigs that house the collagen based microchannel.[92] Before device fabrication, two plexiglass pieces and glass coverslip were bio-functionalized by corona treatment, 10minutes of 1% polyethyleneimine (PEI) coating and followed by rinsing and 30 minutes of 0.1% glutaldehyde treatment. Cold collagen was mixed with bone marrow stromal cells HS27A or HS5 at a final concentration of 10^6 cells/ml on ice. Plasma cleaned polydimethylsiloxane (PDMS, Sylgard 184, Dow-Corning) stamp with microchannel feature was assembled with top plexiglass piece (Figure 4.1A). Two stainless steel dowel pins was placed into the reservoir holed on the top plexiglass piece to block collagen diffusion and create space for inlet and outlet. Stromal cell containing collagen was slowly injected through the injection ports on the top plexiglass piece. Stromal cells containing collagen was dispensed on glass coverslip on the bottom plexiglass piece and covered by a flat PDMS stamp (Figure 4.1B). The dissembled top and bottom plexiglass jigs were then incubated for 30 minutes to allow the solidification of collagen. After collagen solidification, PDMS stamps were removed from both

top and bottom plexiglass pieces. The top part contains microchannel feature and the bottom part forms the bottom of the microchannel. The complete collagen based microchannel network was formed by assembling two plexiglass pieces together and sealed by mechanical pressure (Figure 4.1C). Fresh EGM was then perfused through microchanel for one hour at 37^{o}C in a 5% CO_2 humidified chamber.

4.3.6 Cell seeding and culture

HUVECs were trypisinized and resuspended at a concentration of 5X10^{6} cells/ml. 10ul of HUVECs suspension was added into the inlet of microdevice after removal of media from both inlet and outlet (Figure 4.1C). The HUVECs seeded microdevice was incubated at 37^{o}C for 15 minutes to allow cell attachment (Figure 4.1D). The cell culture media EGM was then added into both inlet and outlet for the first 12 hours. Microdevices were fed every 12 hours by removing media and adding fresh media into inlet.

4.3.7 Immunofluorescence staining

After 3 days of culture, microdevices were fixed in situ by 3.7% formaldehyde for 30 minutes, rinsed three times with phosphate buffered saline (PBS), blocked and permeabilized by PBS containing 2% bovine serum albumin (BSA) and Triton X-100 (Invitrogen), rinsed three times with PBS, and stained with CD31 antibody and counterstained with Hoechst 33342. The immunofluorescence images of microdevices were taken in situ using a Nikon A1R confocal microscope and analyzed with FIJI software.

4.3.8 Scanning electron micrograph

After immunofluorescence images of microdevices were taken, microdevices were re-fixed with glutaldehyde for 20 minutes and rinsed three times with PBS. The microdevices were then dissembled into top and bottom parts. After the microvessels were opened, the thick top parts of microvessel containing collagen were dehydrated in serial ethanol washes (50%, 75%, 85% and 100% ethanol), further dehydrated by critical point drying, sputtered coated with gold-platinum and analyzed by a FEI Sirion scanning electron microscope with an accelerating voltage of 5 kV.

4.3.9 Simulation of flow profiles in microvessel network

Regarding the simulation of flow profiles in the network, the software tool COMSOL Multiphysics® was used. In the simulation, the parameters used were set as follows: all properties of the solution adopted those of water at 293.15K; the inlet pressure was set to be 100 Pa, which was based on the assumption that the liquid height was kept to be 1cm; the outlet pressure was zero. The fluid flow is assumed to be laminar and the following equations are used:

$$\rho(\mathbf{u}\cdot\nabla)\mathbf{u} = \nabla\cdot\left[-p\mathbf{I} + \mu\left(\nabla\mathbf{u} + (\nabla\mathbf{u})^{T}\right) - \frac{2}{3}\mu(\nabla\cdot\mathbf{u})\mathbf{I}\right]$$

$$\nabla\cdot(\rho\mathbf{u}) = 0$$

where ∇ denotes Hamiltonian, T denotes the matrix transpose, u is a velocity vector, ρ is the fluid density, I is a unit vector, p is the pressure and μ is the fluid viscosity.

4.3.10 Statistical Analysis

Data is presented as mean ± standard deviation of the mean and significant differences were determined by independent or paired student t tests. A p value less than 0.05 was considered as significant difference.

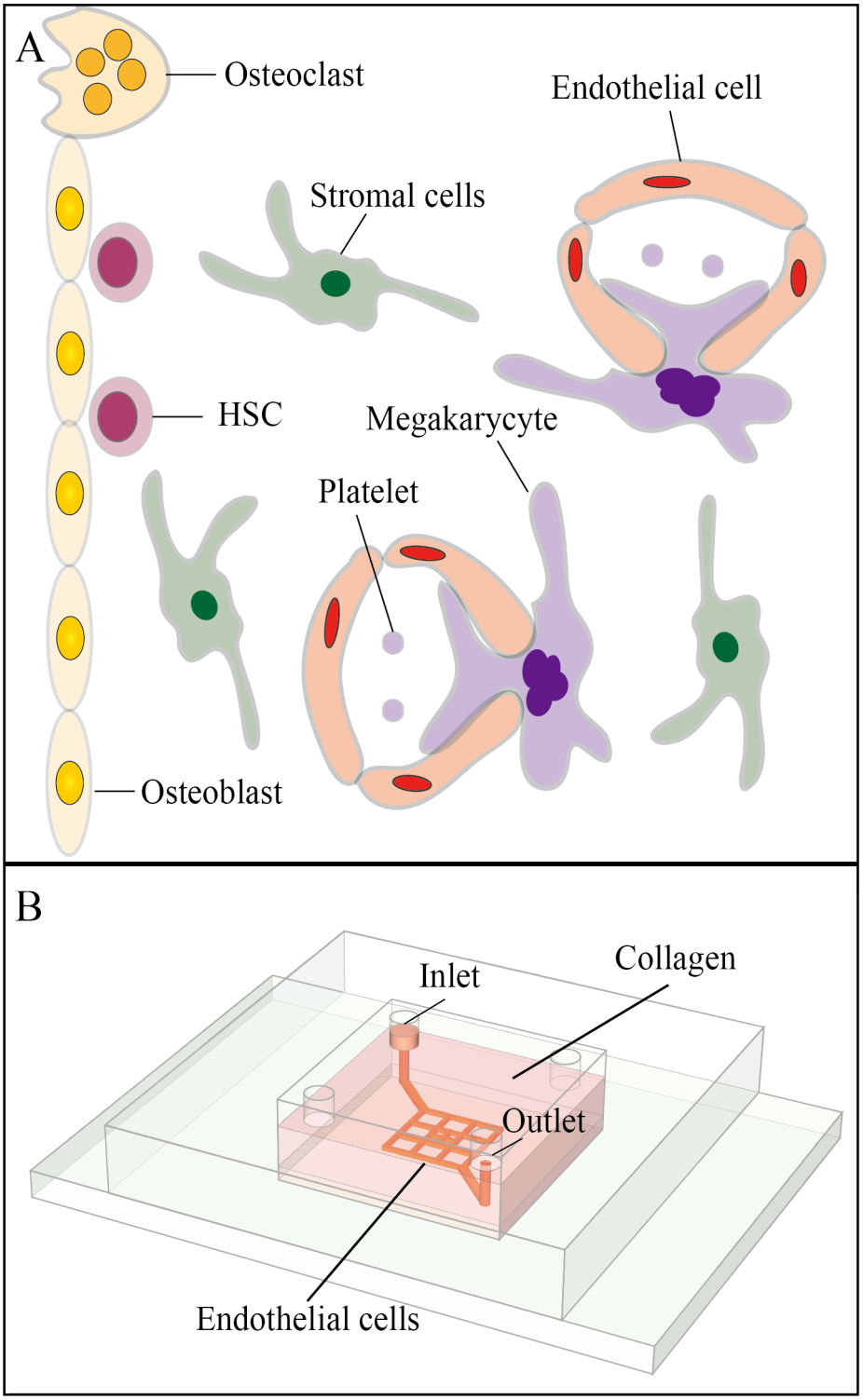

Figure 4.2 Biological inspired design of a bone marrow niche mimic microdevice.

(A) Hematopoietic stem cells (HSCs) locating closed to endosteal niche generate megakaryocyte (MK) progenitor cells that migrate toward sinusoid. Mature MKs release platelets into sinusoidal

blood stream. (B)The microdevice contains a 3-D microvascular network and extracellular matrix (type 1 collagen). Fresh media containing soluble factors was perfused from inlet.

4.4 Results

4.4.1 Establishment of a 3-D microdevice to mimic bone marrow niche for thrombopoiesis

While primitive hematopoietic stem cells reside close to endosteal niche, mature MKs are located less than 1 μm away from the bone marrow sinus wall [94], that allows MKs to either extend proplatelets into bloodstream to release platelets, or migrate through transendothelial apertures to reach the lung. Sinus, perivascular stromal cells and extracelluar matrix constitute the most important parts of microenvironment for thrombopoiesis (Figure 4.2A). Here, we built a 3-D microdevice to mimic bone marrow niche for thrombopoiesis containing a microvascular network, extracellular matrix type 1 collagen and bone marrow stromal cells (Figure 4.2B, Figure 4.1). 10^6 cells/ml stromal cells were mixed with 7.5mg/ml collagen, which provide an appropriate stiffness to allow vessel microstructure and stromal cell attachment [92]. HUVECs were seeded into microchannel and form a microvessel network.

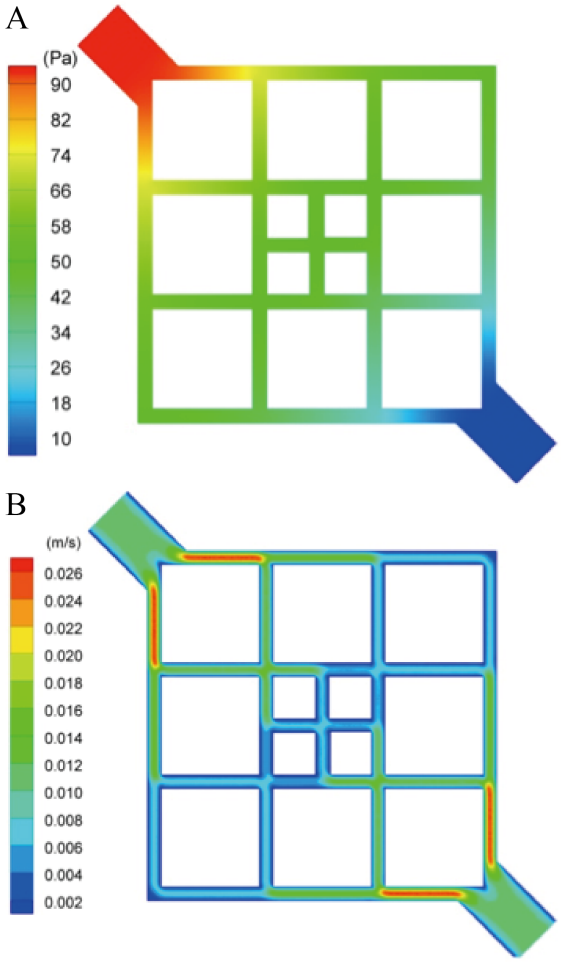

Figure 4.3 Simulation of flow profiles (pressure (A) and flow velocity (B)) in the microvessel network.

The microchannel cross-section was designed as 100μm×100μm; for the big square box, the side length was 700μm×700μm; for the small square box, the side length was 300μm×300μm

To better study the effect of flow rate on microvessel, a branching microchannel network was design. Simulation of flow profiles in the microchannel shows that the pressure decreases along the flow direction from inlet to outlet (Figure 4.3A) whereas the average velocity decreases first and then increases along the direct from the upper left to the lower right due to the change of the

flow cross-section area (Figure 4.3B). Therefore, this network can provide various regions with different velocities for the cell culture.

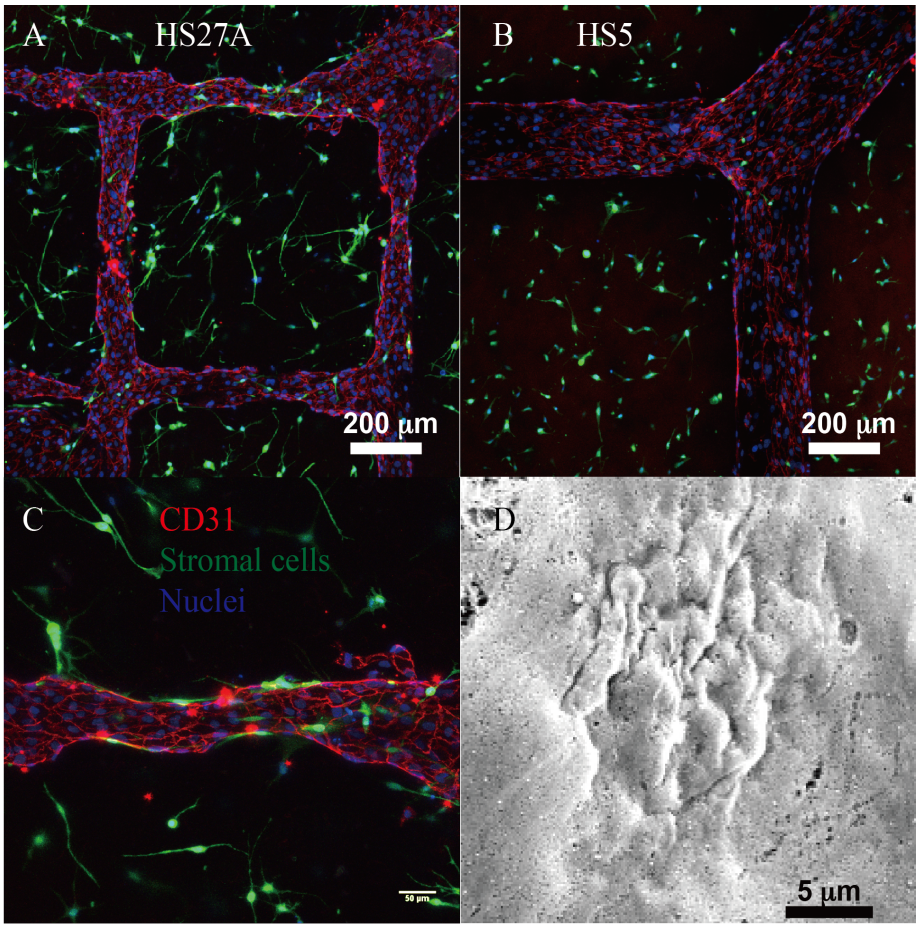

Figure 4.4 Stromal cells and microvessel interaction after 3 days culture in 3D biomimetic microdevice.

(A) Z-stack projection of horizontal confocal sections of HS27A cells and microvessel. (B) Z-stack projection of horizontal confocal sections of HS5 cells and microvessel. (C) Zoom-in confocal sections of HS27A cells and microvessel. A sprouting angiogenesis was formed from microvessel. Red, CD31; Green, stromal cells (HS27A or HS5); Blue, nuclei. (D) Scanning electronic microscopic image showing microvessel lumen after 3 days coculture with HS27A in the 3D biomimic mcirodevice.

4.4.2 Endothelial cell-stromal cell interaction

Two bone marrow stromal cell lines HS27A and HS5 were used to coculutre with microvessel. HS27A could be distinguished roughly by morphology from HS5 – HS27A cells have longer branches of cytoplasm than HS5 have (Figure 4.4A, B). After 3 days culture, HS27A cells lined outside of the microvessel and wrapped around the endothelial cells (Figure 4.4A), while HS5 had limited interaction with microvessel (Figure 4.4B). Wrapped HS27A cells also cause the retraction of the lumen of the microvessel (Figure 4.4D). Sprouting angiogenesis was also occurs when microvessel cocultured with HS27A (Figure 4.4a) and HS5 (Data not shown).

4.5 Discussion

Bone marrow hematopoietic niches are composed of a large number of microenvironmental features, including soluble factors, cell-cell interaction, extracellular matrix and physical support. A good platform to mimic bone marrow niche should meet the following requirements: (a) The *in vitro* niche should be able to mimic the specialized microenvironment for a specific cell type or a specific condition. Although the numerous hematopoietic cells inside bone marrow are crowed within the marrow space, each cell still has its specific niche. Primitive stem cells tend to locate close to endosteal niche, while differentiated cells tend to migrate to the sinus. The study objective was to design an in vitro niche. (b) The niche should be able to precisely control every single viable in it. The most advantage of in vitro niche compared to in vivo niche is that the single viable could unlinked from other factors and precisely controlled.

In this project, the point of interest is to study thrombopoiesis, which determined the most important niche is vascular and perivascular niche. Thus, in this chapter, we present a bone marrow niche for thrombopoiesis that contains a precisely controlled microvessel network,

perivascular stromal cells and extracellular matrix. A number of parameters could be controlled for better understanding of thrombopoiesis: (a) shear stress. By changing the flow velocity using a syringe pump, shear stress could be precisely controlled. (b) microvessel geometry. Microvessel geometry could be changed by changing the top PDMS stamp. In this chapter, a grid network was used to obtain several shear stress and velocity at the same device. (c) matrix cells. Not only stromal cells, other bone marrow cell type, e.g. HSCs, neurons, adipocyte, could also be cocultured in the matrix to study cell-cell interaction. (d) matrix composition. Single matrix protein or combination of several matrix protein could be used to mimic the specific location inside bone marrow. (e) endothelial cell type. HUVECs are the easiest endothelial cells, but not the true endothelial cells in bone marrow. Bone marrow endothelial cell could also be seeded into microdevice. (f) perfused media in the vessel lumen. Zheng et al [92] perfused blood through the microvessel using the similar device to study thrombosis.

In this chapter, two different bone marrow stromal cells HS27A and HS5 were cultured in the perivascular site, displaying different interaction with microvessel. HS27A and HS5 are two bone marrow stromal cells that have very distinct gene profile and function. Morphological, HS-27A cells tend to form a single cell layer, while HS5 cells are lack of contact inhibition [95]. Our result also show that HS27A has longer branches than HS5. HS5 cells release numerous cytokines and support hematopoietic stem cell growth, while HS27A only secret few[95]. However both HS27A and HS5 synthesize vascular endothelial growth factor (VEGF), which explained the sprouting angiogenesis formation of microvessel when either HS27A or HS5 was cultured in the perivascular site. Due to our results that HS27A could wrap around microvessel and the previous study showing the high expression of SDF1[96], HS27A cells could be a pericyte-like cells. HS5 express multiple cytokines genes, extracellular matrix genes and do not

form monolayer[95, 96], indicating that HS5 might be a fibroblast-like cell line. Thus HS27A and HS5 could be used to create two distinct perivascular microenvironment.

In conclusion, a 3-D bone marrow niche biomimetic microdevice was demonstrated in this chapter. This is the platform to study thrombopoiesis in the next chapter. However the application of the biomimetic device could be expanded to by changing one or two parameters in the device. By creating bone marrow hematopoietic niche, a large scale production of hematopoietic cells could be achieved to help clinical transplantation.

Chapter 5 Investigation on interplay between endothelial cells and megakaryocytes

5.1 Abstract

Generating platelets from cord blood is always problematic due to low ploidy of megakaryocytes (MKs) and low numbers of generated platelets, understanding thrombopoiesis from cord blood is urgently needed. The importance of microenvironment on thrombopoiesis has been widely accepted, however, surprisingly little study were about MKs-niche interaction, especially MKs-endothelial cells interaction. One of the reasons is lack of a good *in vitro* model. Using a 3-D bone marrow niche mimic microdevice demonstrated in the previous chapter, we cultured MKs in the perivascular area. MKs migrated toward microvessel and transmigrate across endothelium, leaving fenestration on vessel wall. Sprouting angiogenesis was formed on microvessel. By blocking VEGF signaling, sprouting angiogenesis was inhibited and permeability of microvessel is decreased. Blocking CXCR4 signaling also inhibits micovessel permeability. Further investigation is needed to uncover the mechanism of fenestration.

5.2 Introduction

Mature MKs reside less than 1 μm away from the bone marrow sinus wall allowing platelet shedding into bloodstream[94]. Some MKs pass through the transendothelial apertures, leave bone marrow, reach lung vasculature and release platelets in the lung. Although vascular niche is the most important microenvironment for thrombopoiesis, not many studies focus on the interaction between MKs and endothelial cells. MKs was reported to support the survival of bone marrow endothelial cells and endothelial monolayer promote the proliferation of MKs [97]. The

reported supportive relationship between MKs and endothelial may due to the abundance of pro-angiogenic cytokines produced by MKs and trophic cytokines released by endothelial cells.[98] Here, we investigate the MK-endothelial cell interaction using a 3D co-culture system developed in the previous chapter.

5.3 Materials and methods

5.3.1 Cytokines and antibodies

Recombinant human cytokines interleukin (IL) 3, IL6, SCF and thrombopoietin (TPO) were purchased from R&D Systems (Minneapolis, MN). Phycoerythrin (PE) conjugated anti-human antibodies CD41a and mouse IgG1 isotype control were purchased from BD biosciences (San Jose, CA, http://www.bdbiosciences.com). Rabbit polyclonal CD31 antibody was purchased from Abcam (Cambridge, MA). Hoechst 33342 was purchased from Invitrogen (Grand Island, NY).

5.3.2 Generation of megakaryocytes from umbilical cord blood

As described in previous chapter, human umbilical cord blood (UCB) was donated after obtaining informed consent. UCB was processed by adding 6% (wt/vol) Hetastarch (Hospira, Lake Forest, IL) to a final concentration of 1.2%, and gravity sedimented over 60 min. [51] The leukocyte-enriched supernatant was removed, centrifuged for 10 min at 300 x g, and the leukocyte-poor supernatant was removed. The cell pellet was treated with ACK lysing buffer (Invitrogen, Carlsbad, CA), followed by a wash with PBS. To obtain highly purified CD34+ cells, leukocyte-enriched fractions were labeled with anti-CD34 antibody conjugated to magnetic

microbeads (Miltenyi Biotec, Bergisch Gladbach, Germany). CD34+ cells were positively selected with an autoMACS separator according to the manufacturer's instruction. Greater than 90% of the enriched cells were CD34+ cells as determined by flow cytometry (FACSCaliber; Becton Dickinson).

UCB CD34+ cells were seeded at a density of $5x10^4$ cells/ml and cultured in serum-free X-vivo 10 medium supplemented with a cytokine combination consisting of IL3 (10 ng/ml), IL6 (10 ng/ml), SCF (10 ng/ml), and TPO (50 ng/ml) in 6-well plates. The suspension cultures were incubated and fed every week at 37^{o}C in a 5% CO_2 humidified chamber. After 10 days, cells were collected and stained with PE conjugated CD41a antibody. CD41a+ cells were sorted at >90% purity by BD Biosciences FACSAria III sorter.

5.3.3 Culture of human umbilical vein endothelial cells (HUVECs)

HUVECs (Lonza) were cultured in endothelial cell growth media (EGM, Lonza) at 37^{o}C in a 5% CO_2 humidified chamber. Passages 5 to 6 of HUVECs were used in experiments.

5.3.4 Design and fabrication for 3D biomimetic microdevice

Detailed experiment procedure has been described in the previous chapter. Briefly, CD41+ MKs were mixed with cold 7.5mg/ml collagen containing 100ng/ml TPO, injected into top plexiglass piece and dispensed onto bottom glass coverslip of plexiglass piece. After assemble of top and bottom part of plxiglass, the whole device was perfused with EGM supplementary with 100ng/ml TPO for one hour before endothelial cell seeding.

5.3.5 Cell seeding and culture

HUVECs were trypisinized and resuspended at a concentration of $5X10^6$ cells/ml. 10ul of HUVECs suspension was added into the inlet of microdevice after removal of media from both inlet and outlet. The HUVECs seeded microdevice was incubated at 37^oC for 15 minutes to allow cell attachment. The cell culture media EGM supplemented with 100ng/ml TPO with was then added into both inlet and outlet for the first 12 hours. Microdevices were fed every 12 hours by removing media and adding fresh media into inlet.

5.3.6 Immunofluorescence staining

After 3 days of culture, microdevices were fixed in situ by 3.7% formaldehyde for 30 minutes, rinsed three times with phosphate buffered saline (PBS), blocked and permeabilized by PBS containing 2% bovine serum albumin (BSA) and Triton X-100 (Invitrogen), rinsed three times with PBS, and stained with CD31 antibody and counterstained with Hoechst 33342. The immunofluorescence images of microdevices were taken in situ using a Nikon A1R confocal microscope and analyzed with FIJI software.

5.3.7 Scanning electron micrograph

After immunofluorescence images of microdevices were taken, microdevices were re-fixed with glutaldehyde for 20 minutes and rinsed three times with PBS. The microdevices were then dissembled into top and bottom parts. After the microvessels were opened, the thick top parts of microvessel containing collagen were dehydrated in serial ethanol washes (50%, 75%, 85% and 100% ethanol), further dehydrated by critical point drying, sputtered coated with gold-platinum and analyzed by a FEI Sirion scanning electron microscope with an accelerating voltage of 5 kV.

5.3.8 Measurement of endothelial permeability

To measure the microvessel permeability, I perfused 1cm height of 10uM 40kDa FITC-Dextran (Sigma-Aldrich) from the inlet of the fresh *in situ* fixed microvessel. Fluorescence images were started to be taken by Nikon high resolution fluorescent microscope right before the FITC-dextran was added. Only fluorescence images after 3 minutes were used for permeability analysis by MATLAB(The Mathworks). Under the assumptions: (a) The fluorescence intensity is proportional to the concentration of the fluorescent solute; (b) the concentration within the solution in the microchannels remains constant with respect to both time and the axial position along the channels, the estimated permeability K (μm/s) of microvessel can be estimated as a function of intensity of fluorescent solution, i_0, initial background intensity $i_{initial}$, intensity at the interchannel center i_c, diffusivity of solute in collagen, $D_{collagen}$, interchannel distance δ, and time *t*, according to previous report [92]. We have:

$$ln\frac{i_c - i_0}{i_{initial} - i_0} = -{\lambda_1}^2\frac{D_{collagen}}{\left(\frac{\delta}{2}\right)^2} + ln\frac{4\sin\lambda}{2\lambda_1 + \sin(2\lambda_1)} \quad [1]$$

and

$$K = \frac{D_{collagen}}{\delta/2}\lambda_1 \tan\lambda_1 \quad [2]$$

when λ_n is given by

$$\lambda_n \tan\lambda_n = B_i \quad [3]$$

and B_i is Biot number.

5.4 Results and discussion

5.4.1 Reconstitution of 3D thrombopoietic vascular niche

We reconstituted a 3D vascular niche, which is composed of endothelialized microvascular networks surrounded by the platelet precursors MKs in the type I collagen matrix, to mimic the vascular microenvironment in the marrow for thrombopoiesis (Fig. 5.1). Human MKs were prepared from differentiating hematopoietic CD34+ stem cells, isolated from either human umbilical cord blood or human mobilized peripheral blood (Fig. 5.1B). After 10 days unilineage culture, cord blood derived culture show 69% of cells expressing MK specific marker CD41 (Fig. 5.1C), and peripheral blood culture show 52% CD41+ cells. These CD41+ MKs were purified by flow cytometry and uniformly embedded into collagen gel at 7.5 mg/mL with cell density of 10^6 /mL. A microfluidic circuit was built in the collagen gel via soft lithography and a microvascular network was formed by seeding and culturing human umbilical vein endothelial cells (HUVECs) in the conduit for three to seven days (Fig. 5.1D). The enclosed microvessels enable the perfusion with medium during culture and MKs embedded collagen matrix allow for the close monitoring of them interacting with the microvessels (See the Methods section for details). The co-cultured niche system was maintained for 3-5 days with gravity-driven flow.

After 3 days of culture in growth media, endothelial cells formed junctions at cell-cell contact, indicated by the highly expressed CD31 and VE-cadherins (Fig. 5.1E and 5.1F). Majority of

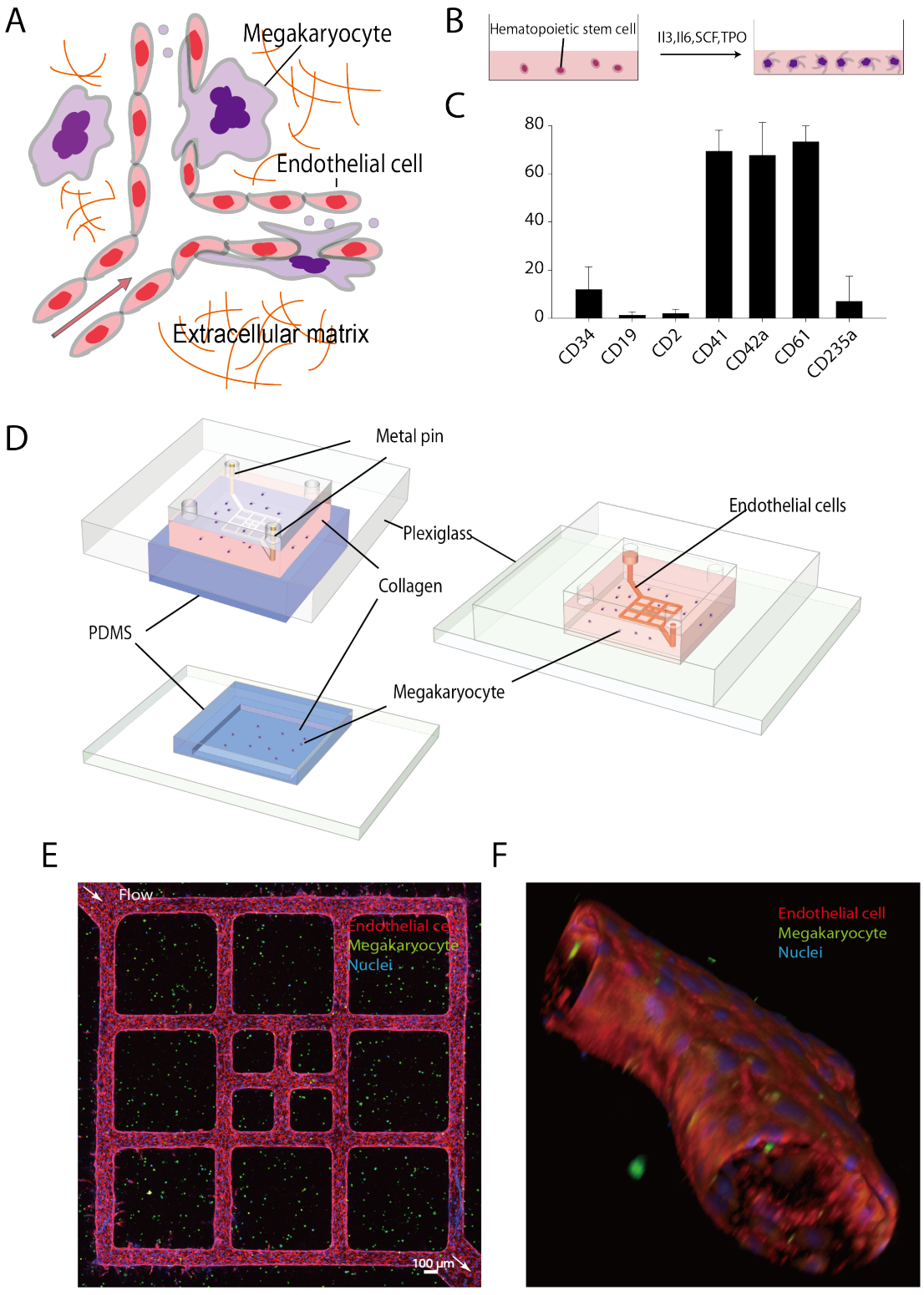

Figure 5.1 **Reconstitution of vascular niche for thrombopoiesis.**

(A) Schematics of megakaryocytes-endothelial cells interaction in bone marrow. (B) Strategy to generate megakarycoytes from human hematopoietic CD34+ cells. (C) Expression of hematopoietic cells surface markers after 10 days culture of human cord blood CD34+ cells. Mean ± S.D., n=4. (D) Schematics of in vitro megakaryocyte (MK) -endothelial cell (EC) coculture system. (E) Z-stack projection of confocal fluorescence imaging of ECs and MKs coculture. Green: CD41 (MK marker); Red: CD31(EC junction marker); Blue: nuclei. (F) 3D reconstitution of confocal fluorescence imaging of ECs and MKs coculture. Green: CD41 (MK marker); Red: CD31(EC junction marker); Blue: nuclei.

CD41+ MKs remained in the matrix, particularly when they were far away from the vessel. Some CD41+ cells resided on abluminal side of microvessel, and some resided inside the microvessel on their luminal surface (Fig. 5.1F).

5.4.2 CXCR4 dependent MK migration and penetration

In the marrow, most of mature MKs locate closed to bone marrow sinusoid, while HSCs residue in osteal niche[99]. Although in vitro study suggested that MKs is capable of migrating toward SDF1a gradient [100-102]and bone marrow endothelial cells express SDF1a it is not clear whether SDF1/CXCR4 dominates the interactions between MKs with microvessels. We combined the live imaging, confocal microscopy, and scanning electron microscopy to clarify this delicate interaction.

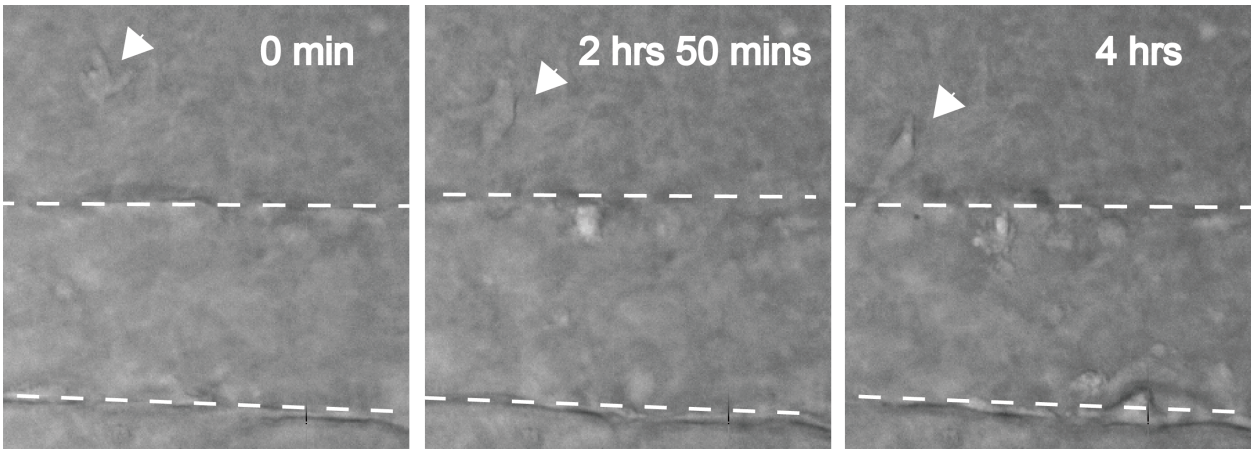

Figure 5.2 A megakaryocyte migrate toward endothelium captured by live imaging microscope.

Arrow: megakaryocyte. Dotted line: endothelium.

With live imaging, we noticed that MKs in the matrix migrated towards the vessel wall (Figure 5.2). After 3 days culture, MK density increased to 3.2 X 10^6 /mL near the vessel wall and decreased to 0. 2 X 10^6 /ml at 300 μm (around 6 times of vessel radii) away from vessel wall (Fig. 5.3), comparing to the original uniform density of 10^6/mL. In contrast, co-culture of bone marrow stromal cells of the same density around microvessels showed no significant change on cell density with respect to the distance to vessel walls over three to seven days of culture (Fig. 5.3B).

When a neutralizing CXCR4 antibody was perfused through the microvessels, there appear to be no spatial difference on MKs density along the distance to vessel wall (Fig. 5.3), indicating the elimination of MK migration by blocking SDF1a-CXCR4 signaling.

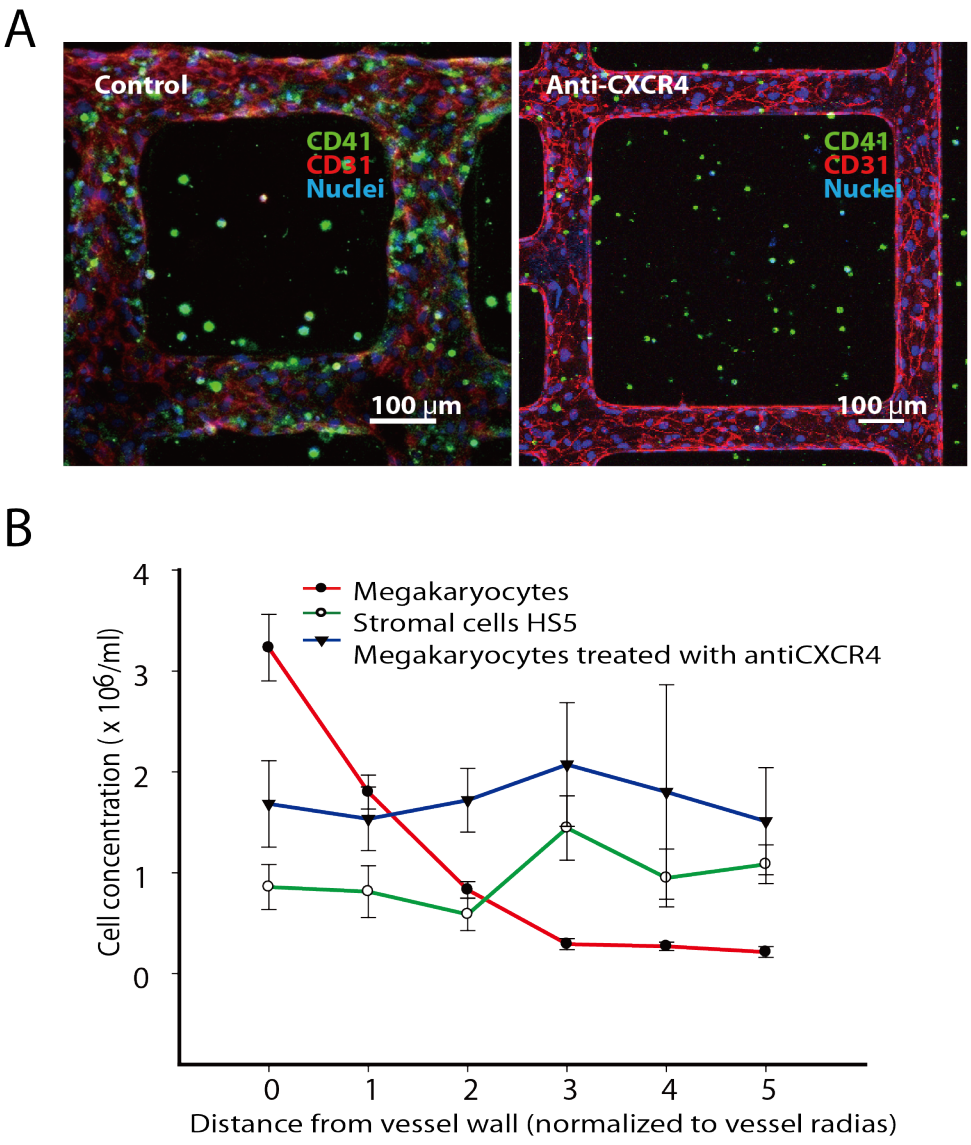

Figure 5.3 Megakaryocytes migrate toward endothelium.

(A) Z-stack projection of confocal fluorescence imaging of ECs and MKs coculture with (right) or without anti-CXCR4 treatment. Green: CD41 (MK marker); Red: CD31 (EC junction marker); Blue: nuclei. (C) Cell density in collagen along the distance to microvessel after 3 days coculture with microvessel.

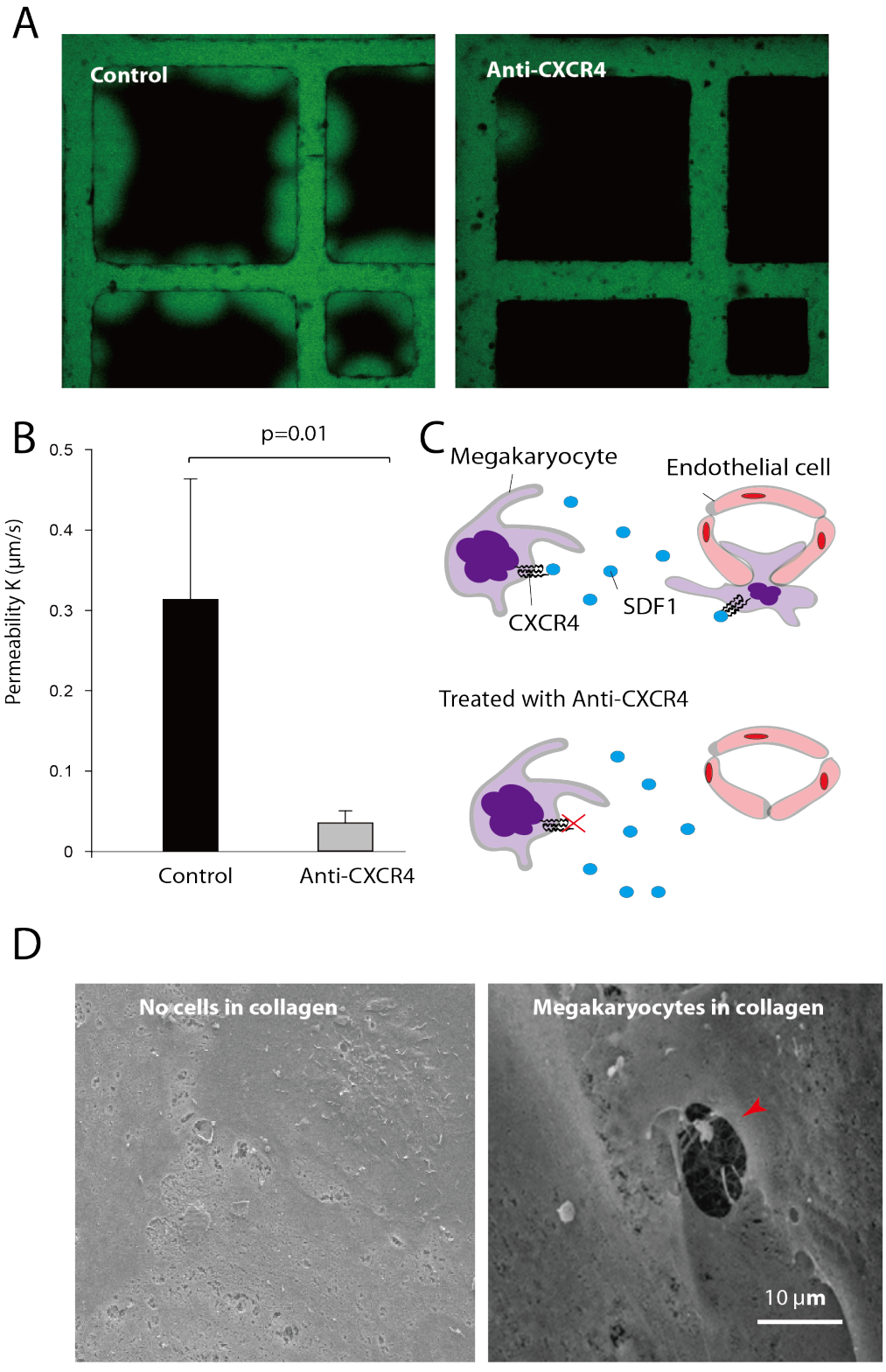

Figure 5.4 CXCR4-dependent of penetration of megakaryocytes

.(A) Fluorescence microscopy of 40kD FITC-Dextran perfusion through microvessel. Left: ECs were cultured in collagen-based microchannel network. Right: ECs were cocultured with MKs in collagen. (B) Permeability analysis of ECs cocultured with MKs in collagen compared to ECs without any cells in collagen. Mean ± S.D., n=3. (C) Schematics of CXCR4-dependent migration and penetration of MKs. (D) SEM of lumen side of microvessel. Left: ECs cultured without any cells in collagen. Middle: ECs cocultured with MKs in collagen. Right: confocal fluorescence imaging of endothelium when MKs were in collagen.

To further assess the effect of MK migration on microvessel, we measured the microvascular permeability through the temporal changes of fluorescence intensity after perfusing FITC conjugated 40kDa Dextran for up to 10 minutes (Fig. 5.4A). When there is no cells in the matrix, microvessels alone had an estimated permeability coefficient, K at 0.047 μm/s; when MKs were co-cultured in the matrix, the vessel permeability coefficient increased to 0.25 μm/s; when CXCR4 antibodies were perfused through the system, the co-cultured vessel permeability 0.09 μm/s which is significantly smaller than the normal co-cultured condition (Fig. 5.4A, B). SEM revealed that pores was left on the vessel wall when microvessel was cocultured with MKs, such pore features may be responsible for the increase of vessel permeability (Fig 5.4C).

5.4.3 Transmigration of MKs and release of proplatelets into microvessels

MKs in the marrow have been shown to release proplatelets into microvessels [103, 104]. However, nothing is known about where on the endothelium and how the MKs penetrated through the vessel wall. We assessed the relative position of MKs and endothelial surfaces and junctions in our system

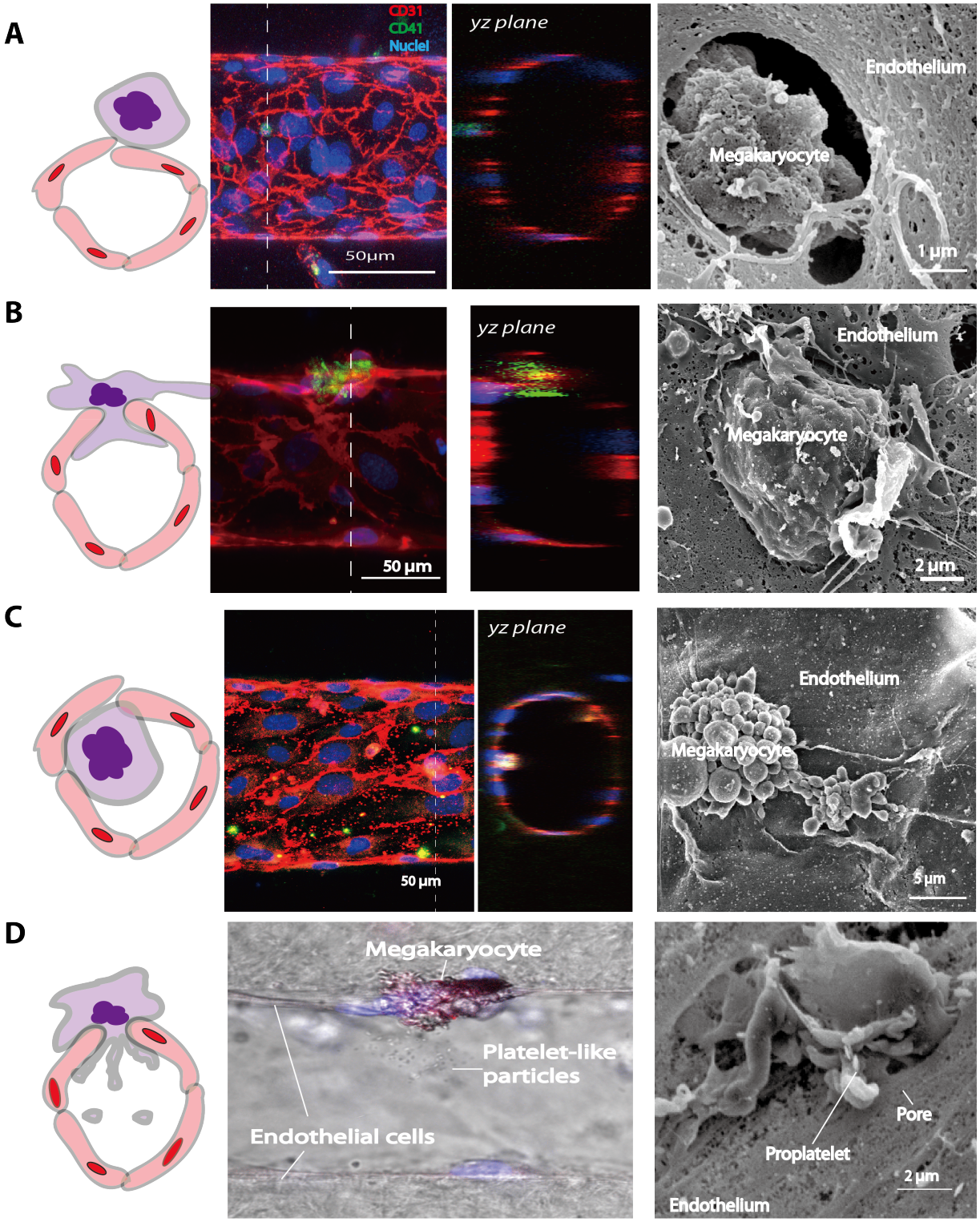
A
CD31
CD41
Nuclei
50μm
yz plane
Endothelium
Megakaryocyte
1 μm
B
50 μm
yz plane
Endothelium
Megakaryocyte
2 μm
C
50 μm
yz plane
Endothelium
Megakaryocyte
5 μm
D
Megakaryocyte
Platelet-like particles
Endothelial cells
Pore
Proplatelet
2 μm
Endothelium

Figure 5.5 Megakaryocytes transmigrate through endothelium or extend proplatelet into microvascular lumen.

Three locations of MKs relative to microvessel: (A) abluminal, (B) transmigrating and (C) luminal. Left column: Schematics of relative position of MKs to microvessel. Middle column: Z-stack projection and yz plane of confocal fluorescence imaging of microvessel and MKs. Right column: SEM imaging showing the position of MKs and endothelium. (D) A megakaryocyte on abluminal surface of microvessel producing platelets into vascular lumen. Left column: Schematics of relative position of MKs to microvessel.. Middle column: Reconstruction of fluorescence and bright field image of a megakaryocyte residing on abluminal surface of microvessel. Red: CD41; Blue: nuclei. Right column: SEM image of a proplatelet protrusion in a pore on endotheloium.

through confocal and scanning electron microscopy (Figs. 5.5). Three different states were observed at the end time point (Fig. 5.5 A-C): (1) abluminal: MKs resided completely on the ablumianl surface of the microvessel (fig. 5.5A); (2) transmigrating: MKs transmigrated across the endothelium and occupied both the abluminal and luminal space (Fig. 5.5B); (3) luminal: MKs completely transmigrated across the endothelium and resided inside the microvessel lumen(fig. 5.5C). Besides the above three states, several MKs residing on abluminal surface of the microvessel directly release platelets into vascular lumen (Fig. 5.5D). SEM also showed three types of particles either penetrating through or residing on luminal vessel wall: (1) proplatelet-like protrusion through the endothelium, indicating the ongoing process of MK transmigration and proplatelet formation (Fig.5.5D), (2) fully migrated MKs in the vessel lumen (Fig. 5.5C), and (3) platelet-like particles and smaller microparticle-size particles in the vessel lumen. These results indicates two different processes occurring in the pores: (1) MKs located on the abluminal

side of microvessel and extended proplatelets through the endothelial pore; and (2) whole MKs or MK fragments transmigrated through the endothelial pore. These transmigrated MKs or MK fragment would probably finalize their maturation in blood vessel and further release platelets in the blood flow. Further confocal and SEM imaging revealed that majorities of MKs transmigrated through endothelium through EC-EC junctions (i.e. paracellular transmigration), and a small amount of MKs transmigrated directly through endothelial membranes (i.e. transcellular transmigration) (Fig. 5.6A,B).

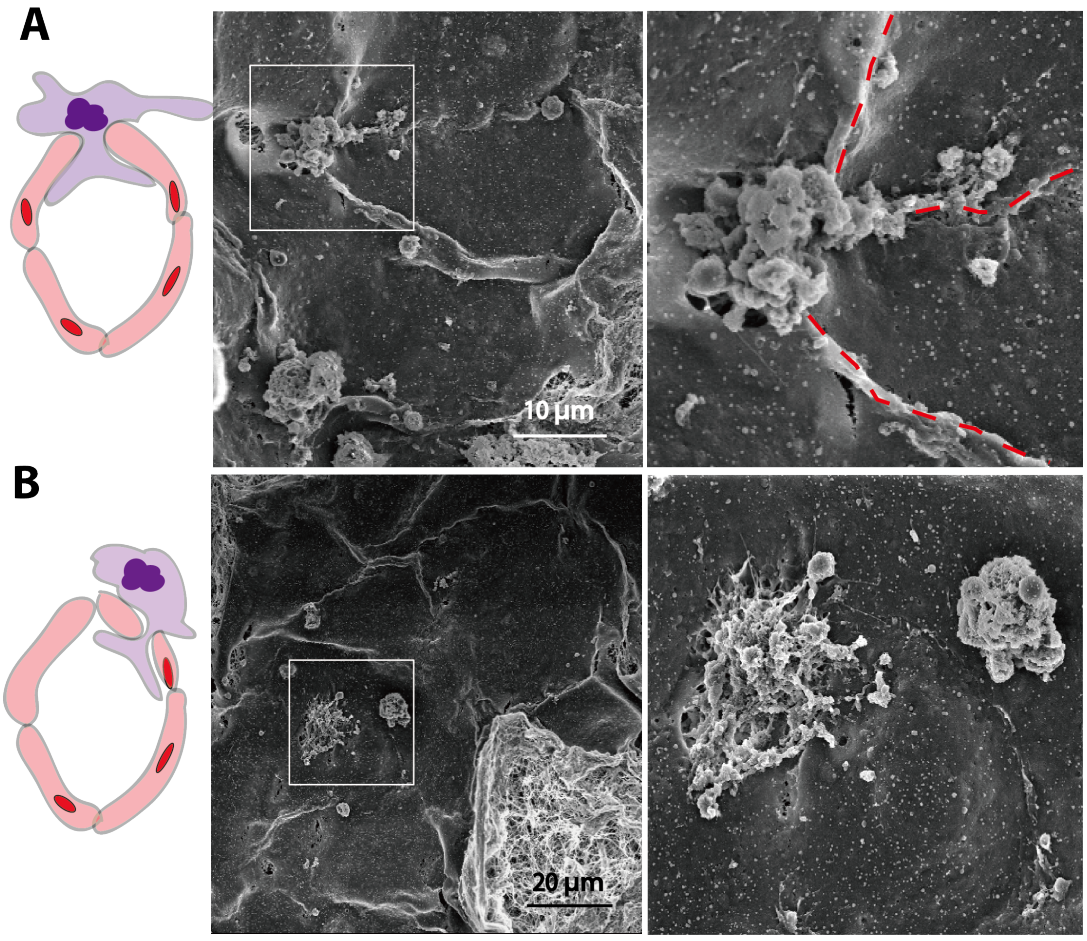

Figure 5.6 Paracellular(A) and intracellular(B) transmigration of MKs through endothelium.

Left column: Schematics of relative position of MKs to endothelial cells. Middle column: SEM images showing the relative position of MKs and endothelial cells. Right column: Enlarged SEM images of middle column.

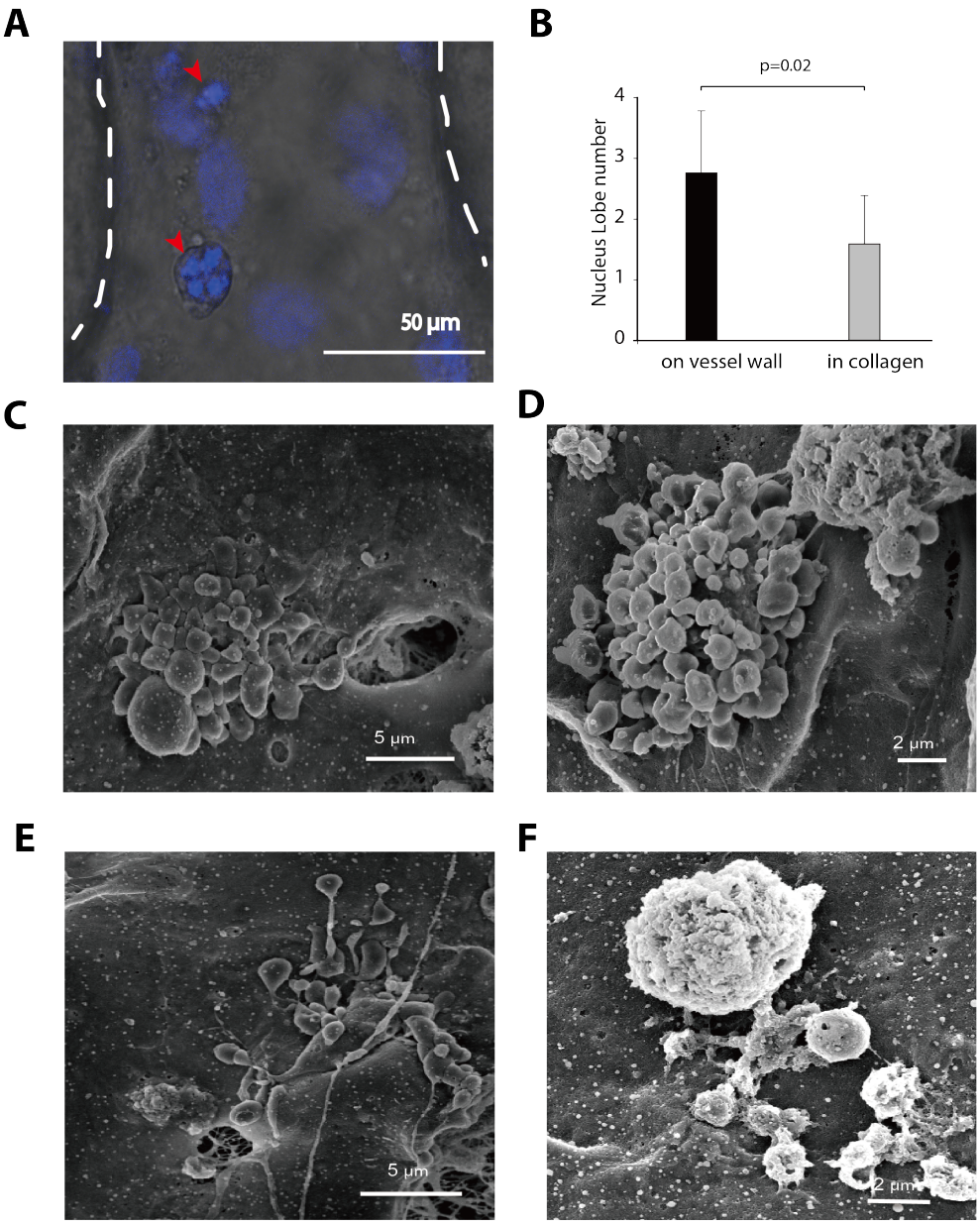

Figure 5.7 Megakaryocytes of different maturation stages in microvessel lumen.

(A) Reconstruction of fluorescence and bright field image showing nucleus of MKs and endothelial cells. Red arrow: MK nucleus. White dotted line: endothelium. (B) Quantification of nucleus lobe number of MKs on vessel wall and in collagen. (C) (D) SEM images showing MKs with platelet territories. (E) SEM image showing proplatelet elongation. (F) SEM image showing naked MK nuclei with few platelets attached.

In the marrow, mature MKs are found to reside near the vasculature and release platelets into the circulation [103, 104]. In our engineered microvascular niche, we examined the maturation stage of MKs around the vasculature and in the vessel lumen. By counting the nuclei lobes in 3D fluorescent images, MKs that are associated with the vessel wall, either migrated or transmigrating, showed higher counts of nuclei lobes compared to MKs far away from the vessel (Fig5.7 A,B). SEM images showed that MKs in the vessel lumen has various differentiation stages (Fig. 5.7 C-F) too: (1) MKs with platelet territories: A MK nuclei like core with a large amount of platelet shaped construction (Fig. 5.7 C, D); (2) Proplatelets: Cytoplasmic elongation with platelet-sized swelling (Fig. 5.7 E); (3) Naked MK nuclei: Small nuclei like structure (Fig. 5.7 F). These different scenarios indicate different stage of MK differentiation towards platelet release.

5.4.4 MKs release functional platelets into microvessel lumen

To determine whether released particles were platelets, we collected the particles and assessed their size distribution and surface markers by flow cytometry. Most of the released particles had similar size as human fresh platelets (fig. 5.8 A, B). We further examined the functions of platelets with a traditional adhesion assay on vWF surface and with a micropost assay for the

platelet contractility during activation. Most of the collected particles adhered and spread on a flat fibrinogen surface after 30 minutes, characterized by formation of lamellipodia (Fig. 5.8 C,D). In the nanopost assay, the collected particles adhered on the VWF or fibrinogen coated nanopost, further contracted with thrombin activation, and deformed nanopost. By measuring the maximal deformation of the adhered nanopost, we measured the total contractile force of a single platelet-like particle is 33.4 nN, which is comparable to the force generated by normal human platelets.

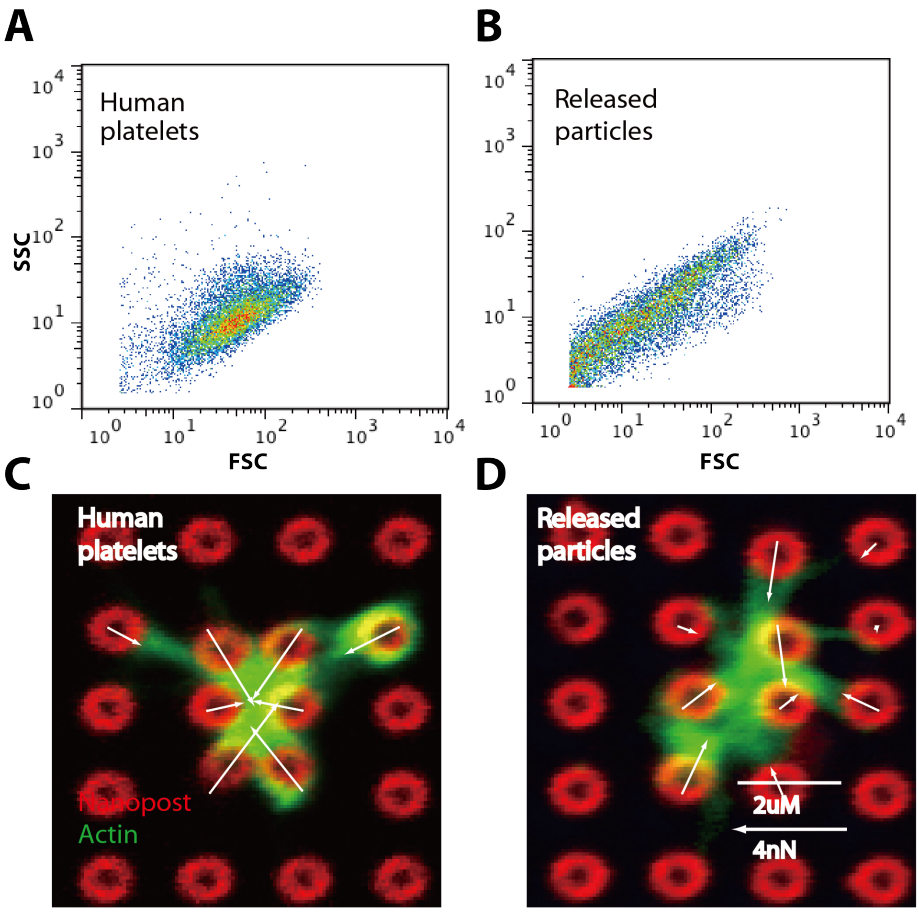

Figure 5.8 Characterization of released platelet-like particles.

(A, B) Flow cytometry analysis of human fresh platelets(A) and culture derived platelet-like particles (B). Dot plot on a log scale showing forward scatter (FSC) and side scatter (SSC). (C, D) Immunofluorescence images of a human platelet (C) and a culture derived platelet-like particles on nanopost. Green: actin; Red: PDMS nanopost; arrow: contractile force.

5.5 Discussion

Here we have developed a 3D marrow vascular niche to study the final maturation and differentiation of megakaryocytes near the marrow vasculature. The system not only allowed us to study the direct interaction between megakaryocytes and endothelial cells, but also unprecedently revealed temporal and spatial changes of MK during the terminal maturation and differentiation to release platelets into the circulation. Bone marrow microvessels has have been shown to be an important niche for the differentiation, maturation, and production of hematopoietic cells [97, 105, 106]. The marrow microvasculature is sinusoidal to allow for blood cells transmigration and production[107]. Our study uncovered the process of MKs migrating towards the vessel wall, creating pores on the endothelium, transmigrating across endothelium and releasing platelets into the circulation. We showed for the first time that endothelial cells from a different source (umbilical cord vein in our scenario, considered as a continuous endothelium with no sinusoids or fenestrae) can be modified by the surrounding MKs to become fenestrated or sinusoidal. The fact that decreasing MK density adjacent to microvessel causes microvessel less leaky suggests that fenestration of HUVECs lining microvessel is caused by MKs. The finding raises an interesting question about endothelial cell plasticity. Endothelial cells all over the body display remarkable structure heterogeneity to meet the different functional need in different tissue [103]. Our finding suggests that the control of microenvironment on the structure and function of endothelial cells.

We also demonstrated for the first time that MKs transmigrated through the pores they generated on the endothelium to finish the terminal differentiation. Majority of the transmigration occurred through cell junctions - paracellularly but a small portion occured through cell membranes - transcellularly. Similar transmigration phenomena has been observed in mesenchymal stem cell [108] and leukocyte [109] when they migrate across the endothelial cells. However what determines the transmigration sites is still unknown. In addition to the sites of transmigration, the stages of transmigrating MKs is also different. Proplatelet-generating MKs were observed during the process of transmigration by SEM. This is consistence with several previous studies showing *in vivo* mice proplatelet elongation from MKs through endothelium[104, 110]. Whole MKs or MK fragments were also observed in the middle of transmigration and in the microvessel lumen, which raised a possibility that these MKs could further mature and be trapped in the pulmonary vascular bed to finish differentiation and platelet release. Reports showed higher platelets number in postpulmonary vessels [111]and MKs in lung vasculature[17].

The mechanism of thrombopoiesis has been under debate for years. Old ultrastructure images indicates the cytoplasm fragmentation of mature MKs in bone marrow[112], while recent works suggest a proplatelet stage with long cytoplasmic extension and beaded structure[104, 110, 113]. The proplatelet would be further extended in blood stream and finally release platelets [110]. Our finding suggests a transit stage between demarcation membrane system and proplatelet formation - MKs with platelet territories. These platelet-like beads are still attached to their mother cell, however is ready to extend with the help of fluid shear force. The platelets would be finally shed from the MKs and only the naked MK nuclei would be left either in the microvessel lumen or albumen side.

Our study has provided a unique system to study the crosstalk between MKs and microvessels and suggest the mechanism of thrombopoiesis in their vascular niche at late stage of differentiation. Future improvement are expected to use the bone marrow sinusoids derived endothelial cells to form microvascualture, with reticular cells and marrow stroma in the matrix to fulfill the full function of thrombopoiesis. With optimization, the system could be potentially scaled up to be a bioreactor to produce platelets in vitro for either therapeutic development or in amount large enough for transfusion.

Chapter 6 Conclusion and future work

6.1 Conclusion

Low yield and questionable quality of *in vitro* platelet production reveal a missing critical factors in megakaryopoiesis and thrombopoiesis. What is it? Is it from bone marrow microenvironment?

One challenge is how to identify novel factors contributing to megakaryopoiesis and thrombopoiesis. In Chapter 3, a system approach has been developed to identify plasma membrane receptor genes that significantly up-regulated as HSCs are induced to become MKs. To validate the approach, 7 of 40 up-regulated transmembrane gene has been selected. 6 of 7 of the plasma membrane receptors were confirmed to have functional roles in MK and platelet development. This is also the first study to show that adiponectin, secreted by adipocytes, inhibit MK colony formation significantly. These studies validate that differentially expressed plasma-membrane receptors identified by our microarray analyses of developing MKs have functional roles in megakaryocytopoiesis and platelet biology. Thus, suggesting that there is a strong likelihood that the remaining 33 of the 40 up-regulated plasma membrane-localized receptors have important biological roles in the function and/or development of MKs and platelets. The creation of a developing MK receptome provides an opportunity for users to identify functional roles for previously uncharacterized matched receptor-ligand systems that integrate a multiplicity of environmental cues that are critical for MK development and platelet biology.

Another challenge is the lack of proper tools to study the interaction between MKs and their bone marrow niche. Traditional 2D suspended culture systems fail to mimic in vivo microenvironment, and animal models too are limited in not being easily amenable to the study

of the individual cellular components in different combinations. In chapter 4 and 5, a 3D microvascular niche has been developed to study the interaction between microvessel and terminal maturation of MKs. with this 3D megakaryocyte/microvessel co-culture system, we show that endothelial cells attract megakaryocytes to migrate towards microvessels through signals from SDF-1 to CXCR4. The megakaryocytes, in turn, induce fenestrations in the microvessels. The fenestrae act as "doors" for the megakaryocytes to enter the vessels, where they experience fluid shear stress to shed platelets from the proplatelet processes or platelet territories. These results demonstrate the usefulness of this system for the study of thrombopoiesis, and the possibility that it can be used to reconstitute the entire marrow microenvironment. Because it is possible to use entirely human components, this system can also be used to screen thrombopoietic drugs, to study disorders of platelet formation and structure, and to potentially be scaled up as a bioreactor to produce functional platelets for transfusion.

6.2 Future work

Megakaryocyte migration, thrombopoiesis and shear stress

The design of microvascular network in our 3D bone marrow niche developed in Chapter 4 and 5 allow different shear stress in the same device. It would be interesting to investigate whether migration of MKs toward endothelium would be controlled by shear stress. In our study, we observed whole MKs transmigrated through endothelium and rolling in the vessel wall and also observe MKs extend proplatelet into circulation. Do these two phenomena also controlled by shear stress? Dunois-Lardé et al applied high shear stress on MKs in a perfusion chamber and found more platelet release under high shear condition[28]. It would be interesting to investigate

in our device whether high shear would promote proplatelet formation and platelet released, and also probably inhibit transmigration of the whole MKs.

Adipocytes and thrombopoiesis

Our study showed that adiponectin is an inhibitor for MK differentiation and ADP induced platelet aggregation. Adiponectin is mainly secreted by adipocytes and interestingly obese persons have lower plasma adiponectin level[74,75]. Given the fact that obese females have significantly elevated platelet count compared with normal weight female[114], the prediction would be production of MK progenitors will decrease as adiponectin levels increase or as body fat content decreases. It would be interesting to test this hypothesis in our 3D bone marrow niche.

References

1. Kaushansky, K., *Historical review: megakaryopoiesis and thrombopoiesis.* Blood, 2008. 111(3): p. 981-6.
2. Ruggeri, Z.M. and G.L. Mendolicchio, *Adhesion Mechanisms in Platelet Function.* Circ Res, 2007. 100(12): p. 1673-1685.
3. Davi, G. and C. Patrono, *Mechanisms of disease: Platelet activation and atherothrombosis.* New England Journal of Medicine, 2007. 357(24): p. 2482-2494.
4. Semple, J.W., J.E. Italiano, Jr., and J. Freedman, *Platelets and the immune continuum.* Nature Reviews Immunology, 2011. 11(4): p. 264-274.
5. Sekhon, S.S. and V. Roy, *Thrombocytopenia in adults: A practical approach to evaluation and management.* Southern Medical Journal, 2006. 99(5): p. 491-498.
6. Geddis, A.E., *Megakaryopoiesis.* Semin Hematol, 2010. 47(3): p. 212-9.
7. Reems, J.A., N. Pineault, and S. Sun, *In vitro megakaryocyte production and platelet biogenesis: state of the art.* Transfus Med Rev, 2010. 24(1): p. 33-43.
8. Deutsch, V.R. and A. Tomer, *Megakaryocyte development and platelet production.* Br J Haematol, 2006. 134(5): p. 453-66.
9. Behnke, O., *An electron microscope study of the rat megacaryocyte. II. Some aspects of platelet release and microtubules.* J Ultrastruct Res, 1969. 26(1): p. 111-29.
10. Thon, J.N. and J.E. Italiano, *Does size matter in platelet production?* Blood, 2012. 120(8): p. 1552-1561.
11. Zucker-Franklin, D. and S. Petursson, *Thrombocytopoiesis--analysis by membrane tracer and freeze-fracture studies on fresh human and cultured mouse megakaryocytes.* J Cell Biol, 1984. 99(2): p. 390-402.

12. Mori, M., J. Tsuchiyama, and S. Okada, *Proliferation, migration and platelet release by megakaryocytes in long-term bone marrow culture in collagen gel.* Cell Struct Funct, 1993. 18(6): p. 409-17.

13. Caine, Y.G., et al., *Adhesion, spreading and fragmentation of human megakaryocytes exposed to subendothelial extracellular matrix: a scanning electron microscopy study.* Scan Electron Microsc, 1986(Pt 3): p. 1087-94.

14. Deutsch, V.R., et al., *The response of cord blood megakaryocyte progenitors to IL-3, IL-6 and aplastic canine serum varies with gestational age.* Br J Haematol, 1995. 89(1): p. 8-16.

15. Eldor, A., et al., *Megakaryocyte interaction with the subendothelial extracellular matrix.* Prog Clin Biol Res, 1986. 215: p. 399-404.

16. Fuentes, R., et al., *Infusion of mature megakaryocytes into mice yields functional platelets.* Journal of Clinical Investigation, 2010. 120(11): p. 3917-22.

17. Zucker-Franklin, D. and C.S. Philipp, *Platelet production in the pulmonary capillary bed - New ultrastructural evidence for an old concept.* American Journal of Pathology, 2000. 157(1): p. 69-74.

18. Kaushansky, K., *The molecular mechanisms that control thrombopoiesis.* Journal of Clinical Investigation, 2005. 115(12): p. 3339-47.

19. Kaushansky, K., et al., *Thrombopoietin expands erythroid progenitors, increases red cell production, and enhances erythroid recovery after myelosuppressive therapy.* Journal of Clinical Investigation, 1995. 96(3): p. 1683-7.

20. Kuter, D.J., D.M. Gminski, and R.D. Rosenberg, *Transforming growth factor beta inhibits megakaryocyte growth and endomitosis.* Blood, 1992. 79(3): p. 619-26.

21. Han, Z.C., S. Bellucci, and J.P. Caen, *Megakaryocytopoiesis: characterization and regulation in normal and pathologic states.* Int J Hematol, 1991. 54(1): p. 3-14.

22. Zauli, G. and L. Catani, *Human megakaryocyte biology and pathophysiology.* Crit Rev Oncol Hematol, 1995. 21(1-3): p. 135-57.

23. Bluteau, D., et al., *Regulation of megakaryocyte maturation and platelet formation.* Journal of Thrombosis and Haemostasis, 2009. 7 Suppl 1: p. 227-34.

24. Massberg, S., et al., *Platelets secrete stromal cell-derived factor 1alpha and recruit bone marrow-derived progenitor cells to arterial thrombi in vivo.* J Exp Med, 2006. 203(5): p. 1221-33.

25. Avecilla, S.T., et al., *Chemokine-mediated interaction of hematopoietic progenitors with the bone marrow vascular niche is required for thrombopoiesis.* Nat Med, 2004. 10(1): p. 64-71.

26. LaIuppa, J.A., E.T. Papoutsakis, and W.M. Miller, *Oxygen tension alters the effects of cytokines on the megakaryocyte, erythrocyte, and granulocyte lineages.* Exp Hematol, 1998. 26(9): p. 835-43.

27. Mostafa, S.S., W.M. Miller, and E.T. Papoutsakis, *Oxygen tension influences the differentiation, maturation and apoptosis of human megakaryocytes.* Br J Haematol, 2000. 111(3): p. 879-89.

28. Dunois-Larde, C., et al., *Exposure of human megakaryocytes to high shear rates accelerates platelet production.* Blood, 2009. 114(9): p. 1875-83.

29. Sabri, S., et al., *Differential regulation of actin stress fiber assembly and proplatelet formation by alpha2beta1 integrin and GPVI in human megakaryocytes.* Blood, 2004. 104(10): p. 3117-25.

30. Balduini, A., et al., *Adhesive receptors, extracellular proteins and myosin IIA orchestrate proplatelet formation by human megakaryocytes.* Journal of Thrombosis and Haemostasis, 2008. 6(11): p. 1900-7.

31. Larson, M.K. and S.P. Watson, *Regulation of proplatelet formation and platelet release by integrin alpha IIb beta3.* Blood, 2006. 108(5): p. 1509-14.

32. Ghevaert, C., et al., *A nonsynonymous SNP in the ITGB3 gene disrupts the conserved membrane-proximal cytoplasmic salt bridge in the alphaIIbbeta3 integrin and cosegregates dominantly with abnormal proplatelet formation and macrothrombocytopenia.* Blood, 2008. 111(7): p. 3407-14.

33. Kato, K., et al., *Genetic deletion of mouse platelet glycoprotein Ibbeta produces a Bernard-Soulier phenotype with increased alpha-granule size.* Blood, 2004. 104(8): p. 2339-44.

34. Poujol, C., et al., *Absence of GPIbalpha is responsible for aberrant membrane development during megakaryocyte maturation: ultrastructural study using a transgenic model.* Exp Hematol, 2002. 30(4): p. 352-60.

35. Bruno, S., et al., *In vitro and in vivo megakaryocyte differentiation of fresh and ex-vivo expanded cord blood cells: rapid and transient megakaryocyte reconstitution.* Haematologica, 2003. 88(4): p. 379-87.

36. De Bruyn, C., et al., *Ex vivo expansion of neutrophil precursor cells from mobilized peripheral blood cells: similar results in cancer patients and normal donors.* Cytotherapy, 2005. 7(6): p. 470-7.

37. Matsunaga, T., et al., *Ex vivo large-scale generation of human platelets from cord blood CD34+ cells.* Stem Cells, 2006. 24(12): p. 2877-87.

38. Proulx, C., et al., *Preferential ex vivo expansion of megakaryocytes from human cord blood CD34+-enriched cells in the presence of thrombopoietin and limiting amounts of stem cell factor and Flt-3 ligand.* J Hematother Stem Cell Res, 2003. 12(2): p. 179-88.

39. Sun, L., et al., *In vitro biological characteristics of human cord blood-derived megakaryocytes.* Ann Acad Med Singapore, 2004. 33(5): p. 570-5.

40. Gandhi, M.J., et al., *A novel strategy for generating platelet-like fragments from megakaryocytic cell lines and human progenitor cells.* Blood Cells Mol Dis, 2005. 35(1): p. 70-3.

41. Guerriero, R., et al., *Unilineage megakaryocytic proliferation and differentiation of purified hematopoietic progenitors in serum-free liquid culture.* Blood, 1995. 86(10): p. 3725-36.

42. Choi, E.S., et al., *Platelets generated in vitro from proplatelet-displaying human megakaryocytes are functional.* Blood, 1995. 85(2): p. 402-13.

43. Norol, F., et al., *Effects of cytokines on platelet production from blood and marrow CD34+ cells.* Blood, 1998. 91(3): p. 830-43.

44. Gaur, M., et al., *Megakaryocytes derived from human embryonic stem cells: a genetically tractable system to study megakaryocytopoiesis and integrin function.* Journal of Thrombosis and Haemostasis, 2006. 4(2): p. 436-42.

45. Takayama, N., et al., *Generation of functional platelets from human embryonic stem cells in vitro via ES-sacs, VEGF-promoted structures that concentrate hematopoietic progenitors.* Blood, 2008. 111(11): p. 5298-306.

46. Sullenbarger, B., et al., *Prolonged continuous in vitro human platelet production using three-dimensional scaffolds.* Exp Hematol, 2009. 37(1): p. 101-10.

47. Pallotta, I., et al., *Three-dimensional system for the in vitro study of megakaryocytes and functional platelet production using silk-based vascular tubes.* Tissue Eng Part C Methods, 2011. 17(12): p. 1223-32.

48. Xi, J., et al., *Infusion of megakaryocytic progenitor products generated from cord blood hematopoietic stem/progenitor cells: results of the phase 1 study.* PLoS One, 2013. 8(2): p. e54941.

49. Thon, J.N. and J.E. Italiano, *Platelet formation.* Semin Hematol, 2010. 47(3): p. 220-6.

50. Chen, J., et al., *N-acetylcysteine reduces the size and activity of von Willebrand factor in human plasma and mice.* Journal of Clinical Investigation, 2011. 121(2): p. 593-603.

51. Rubinstein, P., et al., *Processing and cryopreservation of placental/umbilical cord blood for unrelated bone marrow reconstitution.* Proc Natl Acad Sci U S A, 1995. 92(22): p. 10119-22.

52. Levine, R.F., K.C. Hazzard, and J.D. Lamberg, *The significance of megakaryocyte size.* Blood, 1982. 60(5): p. 1122-31.

53. Stenberg, P.E. and J. Levin, *Mechanisms of platelet production.* Blood Cells, 1989. 15(1): p. 23-47.

54. Liu, Z.J., et al., *Developmental differences in megakaryocytopoiesis are associated with up-regulated TPO signaling through mTOR and elevated GATA-1 levels in neonatal megakaryocytes.* Blood, 2011. 117(15): p. 4106-17.

55. Ignatz, M., et al., *Umbilical cord blood produces small megakaryocytes after transplantation.* Biol Blood Marrow Transplant, 2007. 13(2): p. 145-50.

56. Liu, Z.J. and M. Sola-Visner, *Neonatal and adult megakaryopoiesis.* Curr Opin Hematol, 2011. 18(5): p. 330-7.

57. Mattia, G., et al., *Different ploidy levels of megakaryocytes generated from peripheral or cord blood CD34+ cells are correlated with different levels of platelet release.* Blood, 2002. 99(3): p. 888-97.

58. Slayton, W.B., et al., *Developmental differences in megakaryocyte maturation are determined by the microenvironment.* Stem Cells, 2005. 23(9): p. 1400-8.

59. Sola-Visner, M.C., et al., *Megakaryocyte size and concentration in the bone marrow of thrombocytopenic and nonthrombocytopenic neonates.* Pediatr Res, 2007. 61(4): p. 479-84.

60. Schulze, H. and R.A. Shivdasani, *Mechanisms of thrombopoiesis.* J Thromb Haemost, 2005. 3(8): p. 1717-24.

61. Shim, M.H., et al., *Gene expression profile of primary human CD34+CD38lo cells differentiating along the megakaryocyte lineage.* Exp Hematol, 2004. 32(7): p. 638-48.

62. Reems, J.A. and B. Torok-Storb, *Cell cycle and functional differences between CD34+/CD38hi and CD34+/38lo human marrow cells after in vitro cytokine exposure.* Blood, 1995. 85(6): p. 1480-7.

63. Chen, J., et al., *ToppGene Suite for gene list enrichment analysis and candidate gene prioritization.* Nucleic Acids Res, 2009. 37(Web Server issue): p. W305-11.

64. Ben-Shlomo, I., et al., *Signaling receptome: a genomic and evolutionary perspective of plasma membrane receptors involved in signal transduction.* Sci STKE, 2003. 2003(187): p. RE9.

65. Lara-Castro, C., et al., *Adiponectin and the metabolic syndrome: mechanisms mediating risk for metabolic and cardiovascular disease.* Curr Opin Lipidol, 2007. 18(3): p. 263-70.

66. Yokota, T., et al., *Paracrine regulation of fat cell formation in bone marrow cultures via adiponectin and prostaglandins.* J Clin Invest, 2002. 109(10): p. 1303-10.

67. DiMascio, L., et al., *Identification of adiponectin as a novel hemopoietic stem cell growth factor.* J Immunol, 2007. 178(6): p. 3511-20.

68. Diez, J.J. and P. Iglesias, *The role of the novel adipocyte-derived hormone adiponectin in human disease.* Eur J Endocrinol, 2003. 148(3): p. 293-300.

69. Ukkola, O. and M. Santaniemi, *Adiponectin: a link between excess adiposity and associated comorbidities?* J Mol Med, 2002. 80(11): p. 696-702.

70. Avcu, F., et al., *Association of plasma adiponectin concentrations with chronic lymphocytic leukemia and myeloproliferative diseases.* Int J Hematol, 2006. 83(3): p. 254-8.

71. Molica, S., et al., *Prognostic relevance of serum levels and cellular expression of adiponectin in B-cell chronic lymphocytic leukemia.* Int J Hematol, 2008. 88(4): p. 374-80.

72. Crawford, L.J., et al., *Adiponectin is produced by lymphocytes and is a negative regulator of granulopoiesis.* J Leukoc Biol, 2010. 88(4): p. 807-11.

73. Pineiro, R., et al., *Adiponectin is synthesized and secreted by human and murine cardiomyocytes.* FEBS Lett, 2005. 579(23): p. 5163-9.

74. Yokota, T., et al., *Adiponectin, a new member of the family of soluble defense collagens, negatively regulates the growth of myelomonocytic progenitors and the functions of macrophages.* Blood, 2000. 96(5): p. 1723-32.

75. Berner, H.S., et al., *Adiponectin and its receptors are expressed in bone-forming cells.* Bone, 2004. 35(4): p. 842-9.

76. Katsiougiannis, S., et al., *Salivary gland epithelial cells: a new source of the immunoregulatory hormone adiponectin.* Arthritis Rheum, 2006. 54(7): p. 2295-9.

77. Miller, M., et al., *Adiponectin and functional adiponectin receptor 1 are expressed by airway epithelial cells in chronic obstructive pulmonary disease.* J Immunol, 2009. 182(1): p. 684-91.

78. Gimble, J.M., et al., *The function of adipocytes in the bone marrow stroma: an update.* Bone, 1996. 19(5): p. 421-8.

79. Richardson, R.L., et al., *Transforming growth factor type beta (TGF-beta) and adipogenesis in pigs.* J Anim Sci, 1989. 67(8): p. 2171-80.

80. Hotamisligil, G.S., N.S. Shargill, and B.M. Spiegelman, *Adipose expression of tumor necrosis factor-alpha: direct role in obesity-linked insulin resistance.* Science, 1993. 259(5091): p. 87-91.

81. Horn, P., et al., *Impact of individual platelet lysates on isolation and growth of human mesenchymal stromal cells.* Cytotherapy, 2010. 12(7): p. 888-98.

82. Sakamaki, S., et al., *Transforming growth factor-beta1 (TGF-beta1) induces thrombopoietin from bone marrow stromal cells, which stimulates the expression of TGF-beta receptor on megakaryocytes and, in turn, renders them susceptible to suppression by TGF-beta itself with high specificity.* Blood, 1999. 94(6): p. 1961-70.

83. Greenberg, S.M., et al., *Transforming growth factor beta inhibits endomitosis in the Dami human megakaryocytic cell line.* Blood, 1990. 76(3): p. 533-7.

84. Yu, Q. and I. Stamenkovic, *Cell surface-localized matrix metalloproteinase-9 proteolytically activates TGF-beta and promotes tumor invasion and angiogenesis.* Genes Dev, 2000. 14(2): p. 163-76.

85. Schultz-Cherry, S. and J.E. Murphy-Ullrich, *Thrombospondin causes activation of latent transforming growth factor-beta secreted by endothelial cells by a novel mechanism.* J Cell Biol, 1993. 122(4): p. 923-32.

86. Miyajima, A., et al., *Receptors for granulocyte-macrophage colony-stimulating factor, interleukin-3, and interleukin-5.* Blood, 1993. 82(7): p. 1960-74.

87. Mazur, E.M., et al., *Modest stimulatory effect of recombinant human GM-CSF on colony growth from peripheral blood human megakaryocyte progenitor cells.* Exp Hematol, 1987. 15(11): p. 1128-33.

88. Chen, S., et al., *[Effect of GM-CSF on expansion and differentiation of CD34+ megakaryocyte progenitor cells from cord blood in vitro]*. Zhongguo Shi Yan Xue Ye Xue Za Zhi, 2005. 13(6): p. 1041-3.

89. Burgess, A.W., J. Camakaris, and D. Metcalf, *Purification and properties of colony-stimulating factor from mouse lung-conditioned medium.* J Biol Chem, 1977. 252(6): p. 1998-2003.

90. Kaplan, A., et al., *The effect of hematopoietic growth factors on platelet aggregability.* Clin Appl Thromb Hemost, 1998. 4(4): p. 238-242.

91. Wang, L.D. and A.J. Wagers, *Dynamic niches in the origination and differentiation of haematopoietic stem cells.* Nat Rev Mol Cell Biol, 2011. 12(10): p. 643-55.

92. Zheng, Y., et al., *In vitro microvessels for the study of angiogenesis and thrombosis.* Proc Natl Acad Sci U S A, 2012. 109(24): p. 9342-7.

93. Iwata, M., et al., *Interleukin-1 (IL-1) inhibits growth of cytomegalovirus in human marrow stromal cells: inhibition is reversed upon removal of IL-1.* Blood, 1999. 94(2): p. 572-8.

94. Lichtman, M.A., et al., *Parasinusoidal location of megakaryocytes in marrow: a determinant of platelet release.* Am J Hematol, 1978. 4(4): p. 303-12.

95. Torok-Storb, B., et al., *Dissecting the marrow microenvironment.* Ann N Y Acad Sci, 1999. 872: p. 164-70.

96. Graf, L., M. Iwata, and B. Torok-Storb, *Gene expression profiling of the functionally distinct human bone marrow stromal cell lines HS-5 and HS-27a.* Blood, 2002. 100(4): p. 1509-11.

97. Rafii, S., et al., *Human bone marrow microvascular endothelial cells support long-term proliferation and differentiation of myeloid and megakaryocytic progenitors.* Blood, 1995. 86(9): p. 3353-63.

98. Nachman, R.L. and S. Rafii, *Platelets, petechiae, and preservation of the vascular wall.* N Engl J Med, 2008. 359(12): p. 1261-70.

99. Calvi, L.M., et al., *Osteoblastic cells regulate the haematopoietic stem cell niche.* Nature, 2003. 425(6960): p. 841-6.

100. Hamada, T., et al., *Transendothelial migration of megakaryocytes in response to stromal cell-derived factor 1 (SDF-1) enhances platelet formation.* J Exp Med, 1998. 188(3): p. 539-48.

101. Kowalska, M.A., et al., *Megakaryocyte precursors, megakaryocytes and platelets express the HIV co-receptor CXCR4 on their surface: determination of response to stromal-derived factor-1 by megakaryocytes and platelets.* Br J Haematol, 1999. 104(2): p. 220-9.

102. Yun, H.J. and D.Y. Jo, *Production of stromal cell-derived factor-1 (SDF-1)and expression of CXCR4 in human bone marrow endothelial cells.* J Korean Med Sci, 2003. 18(5): p. 679-85.

103. Zhang, L., et al., *Sphingosine kinase 2 (Sphk2) regulates platelet biogenesis by providing intracellular sphingosine 1-phosphate (S1P).* Blood, 2013. 122(5): p. 791-802.

104. Junt, T., et al., *Dynamic visualization of thrombopoiesis within bone marrow.* Science, 2007. 317(5845): p. 1767-70.

105. Wilson, A. and A. Trumpp, *Bone-marrow haematopoietic-stem-cell niches.* Nature Reviews Immunology, 2006. 6(2): p. 93-106.

106. Li, W., et al., *Hematopoietic stem cell repopulating ability can be maintained in vitro by some primary endothelial cells.* Exp Hematol, 2004. 32(12): p. 1226-37.

107. Panuganti, S., et al., *Three-stage ex vivo expansion of high-ploidy megakaryocytic cells: toward large-scale platelet production.* Tissue Eng Part A, 2013. 19(7-8): p. 998-1014.

108. Teo, G.S., et al., *Mesenchymal stem cells transmigrate between and directly through tumor necrosis factor-alpha-activated endothelial cells via both leukocyte-like and novel mechanisms.* Stem Cells, 2012. 30(11): p. 2472-86.

109. Muller, W.A., *Mechanisms of leukocyte transendothelial migration.* Annu Rev Pathol, 2011. 6: p. 323-44.

110. Zhang, L., et al., *A novel role of sphingosine 1-phosphate receptor S1pr1 in mouse thrombopoiesis.* J Exp Med, 2012. 209(12): p. 2165-81.

111. Bartley, T.D., et al., *Identification and cloning of a megakaryocyte growth and development factor that is a ligand for the cytokine receptor Mpl.* Cell, 1994. 77(7): p. 1117-24.

112. Kosaki, G. and J. Kambayashi, *Thrombocytogenesis by megakaryocyte; Interpretation by protoplatelet hypothesis.* Proceedings of the Japan Academy Series B-Physical and Biological Sciences, 2011. 87(5): p. 254-272.

113. Lambert, M.P. and M. Poncz, *They're not your daddy's inherited platelet disorders anymore.* Journal of Thrombosis and Haemostasis, 2013. 11(11): p. 2037-8.

114. Samocha-Bonet, D., et al., *Platelet counts and platelet activation markers in obese subjects.* Mediators Inflamm, 2008. 2008: p. 834153.